Master Thesis

Effect of alkalisation on the adhesion of flax fibres - Study on the feasibility of the single fibre fragmentation test

Vincent C. van 't Laar

Delft University of Technology

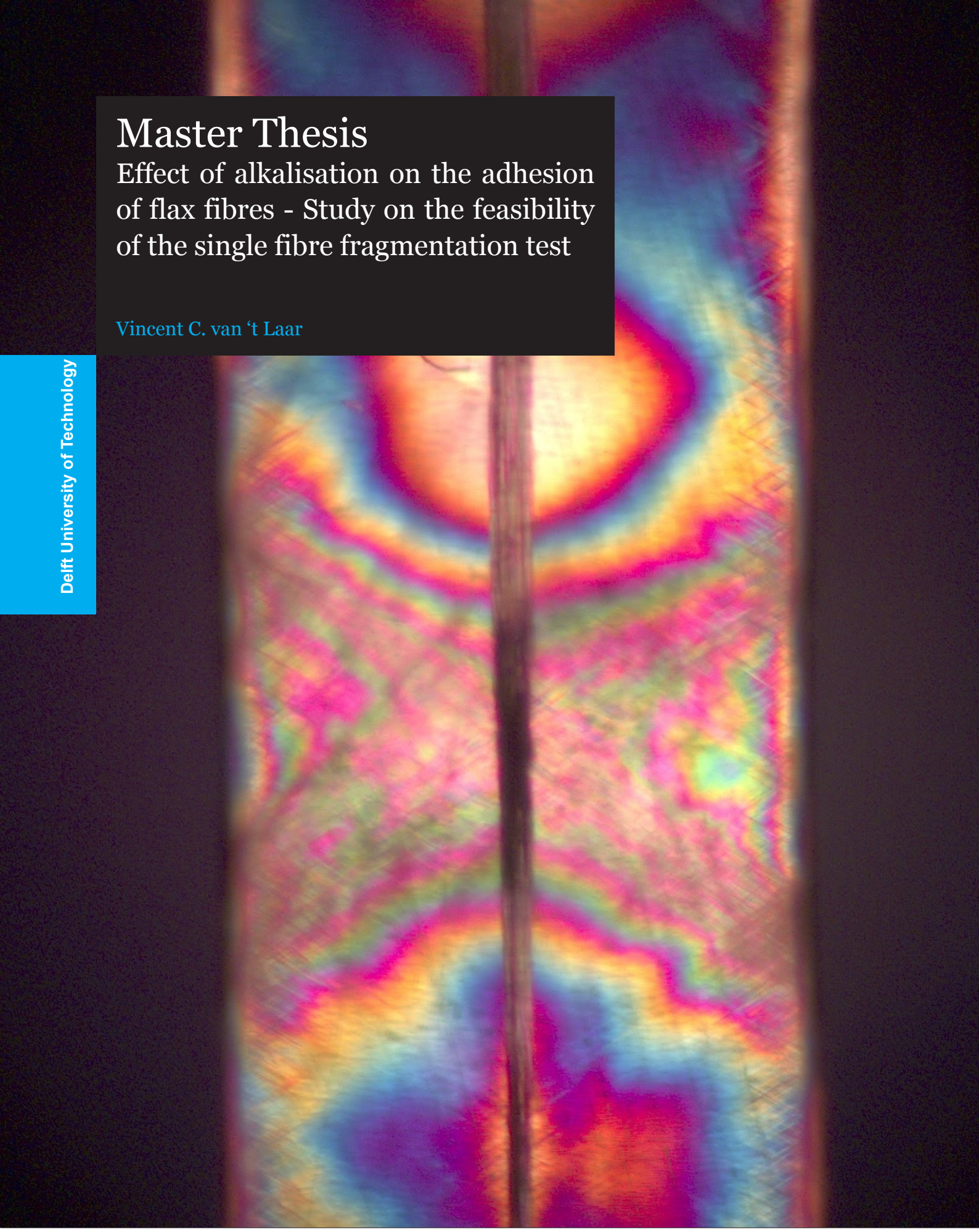

TU Delft Delft University of Technology

Challenge the future

April 7, 2020

Master Thesis

Effect of alkalisation on the adhesion of flax fibres - Study on the feasibility of the single fibre fragmentation test

by

Vincent C. van ‘t Laar

in partial fulfilment of the requirements for the degree of

Master of Science
in Aerospace Engineering

with annotation
in Technology in Sustainable Development

at the Delft University of Technology
to be defended online on Thursday April 16, 2020 at 15:00.

Student number:	4144481	
Chair:	Prof. Clemens A. Dransveld	TU Delft
Supervisor:	Dr. Ir. Julie Teuwen	TU Delft
External:	Dr. Ir. Johan C. Bijleveld	TU Delft

An electronic version of this thesis is available at http://repository.tudelft.nl/.

TU Delft Delft University of Technology

Preface

This thesis was written in fulfilment of the requirements for the degree in Master of Science in Aerospace Engineering - Structures & Materials at the Delft University of Technology with annotation in Technology in Sustainable Development. The topic was chosen out of my personal interest in the field of sustainable materials and their potential application on the market. I would like to use this preface to thank my family for standing by me through think and thin. I would especially like to thank Dr. Ir. Julie Teuwen, for being the best supervisor I could have asked for and for constantly pointing me towards the light at the end of the tunnel whenever I felt overwhelmed and lost. Her patience with me has been commendable.

P.S.: Graduating in the midst of the Covid-19 pandemic will definitely be something I'll never forget.

– "10 voor planning toch?" –

Abstract

In the past decades extreme weather events have become more common as a result of climate change, which is brought on by the increasing concentrations of greenhouse gasses in the atmosphere. Climate change and sustainable development are motivators for the research topic of this thesis, since the prevention of a climate crisis is favourable to the mitigation of its consequences. Emissions and plastic waste can, in part, be decreased by substituting synthetic materials with degradable and sustainably sourced ones since their embodied energy is lower than that of synthetic materials. Flax fibre composites are thought to be capable of competing with glass fibre in various product applications, such as non-essential structures, sports equipment and designer products. Because of the hydrophilic nature of plant fibres, they tend to be subject to incompatibility when paired with hydrophobic polymers such as epoxy, which ultimately means that they have below average interfacial properties. The studies performed on this issue suggest that hydrolysation of the hydrophilic hemicellulose, which is a one of compounds making up plant fibres, with dilute alkali solutions leads to an increment in tensile and transverse properties of flax fibre composites. The interfacial properties of synthetic fibres are best evaluated by performing the pull-out test, the micro-bond test and the single fibre fragmentation test. Since plant fibres are prone to scattered tensile properties, the single fibre fragmentation test is found to be most suitable as it consists of a fully epoxy embedded fibre, increasing the chances of the test to succeed. According to literature, an increase in adhesion manifests as an increased amount fibre fragments in the sample, as well as shorter fragmentation length. Due to the more ductile nature of elementary flax fibre bundles, their fragmentation did not resemble the one observed for synthetic fibres in literature. It was however noticed that the birefringence patterns forming as a consequence of stress concentration, matrix cracks or debonding, could be used as a qualitative indication towards the improvement or deterioration of the interfacial properties. Results were affected by the uncontrollability of independent variables such as fibre diameter, the presence of kink-bands and other naturally occurring fibre defects. Alkalisation was found to affect the birefringence patterns in the single fibre fragmentation test in two opposing ways: by affection adhesion and fibre failure strain. Low intensity treatments showed and increased manifestation of birefringence patterns due to the improved adhesion, while the higher intensity treatments were found to hinder the nucleation and propagation of birefringence patterns because of the decreased failure strain difference between the two materials. Tensile tests of the technical fibres showed that higher intensity treatments led to an increase in failure strain of the fibres due to decrease in micro-fibril angle in elementary fibre bundles and swelling in technical fibres. The applicability of the single fibre fragmentation test in combination with elementary flax fibre bundles is limited due to the hardly controllable independent variables, and is unlikely to provide an accurate quantification of the interfacial shear strength of plant fibres.

Contents

List of Tables

List of Figures

List of Symbols and Abbreviations

Roman Symbols

A_{eff}	Effective load-bearing cross-sectional area of a tachnical fibre	mm^2
F	Force	N
F_0	Force measured by load cell after pre-tension	N
$F_{\max}$	Maximum force	N
L_0	Aperture of the extensometer after pre-tension	mm
N	Amount of data-points within one bin-width	–
x_i	i^{th} data-point within a strain bin-width	mm or %

Greek Symbols

ΔL	Displacement measured by extensometer	mm
ϵ	Percentage strain	%
μ_b	Debond length of the trend line for standard deviation	mm or %
σ	Stress	Pa
σ_c	Tensile strength	Pa
σ_p	Polpulation standard deviation within a strain bin-width	mm or %
σ_t	Tensile stress	Pa

Abbreviations

BRFP	Birefringence pattern
EFB	Elementary fibre bundle
FRP	Fibre reinforced polymer
IFSS	Interfacial shear strength
IPCC	Intergovernmental Panel on Climate Change
MFA	Micro-fibril angle
RFC	Reason for concern
SFFT	Single fibre fragmentation test
TF	Technical fibre
UD	Unidirectional

1

Fibres, composites, their history and climate change

In the past decades composites have gained popularity over metals and other materials due to their high strength, low weight and formability. The raising popularity of these synthetic materials in various industries has led to a substantial increase in research with regards to their mechanical properties and material behaviours. Since their discovery, applications for synthetic materials have been continuously increasing, inevitably replacing more traditional naturally sourced materials. In an ironic sense, it may be said that the biggest strength of synthetic materials is also their biggest weakness: they are so resistant that it is virtually impossible to break them down and revert them to their base molecules. Every kilogram of plastic made, is one more kilogram of plastic that will not degrade in the foreseeable future. Concern for the environment and the health of our planet is a major motivator for the field of study of this thesis: flax fibres and their modification to improve the adhesive properties with the polymer matrix.

1.1. The history of fibres and composites

Mankind has been relying on fibres and composites for a wide use of applications such as textiles, binding materials, construction and hunting for millennia. In more recent years, fibre/polymer composites have emerged. A fibre reinforced polymer is most commonly composed of a synthetic fibre (such as carbon, glass or aramid) embedded in a polymer matrix. The two materials interact through their area of contact, the interface, in such a way that their combined performance exceeds the individual properties of either material.

1.1.1. Fibres: from the caves to the skies

Up until the discovery of plastics, natural fibres were the only type of fibre our ancestors could rely upon. Natural fibres can be classified into three categories depending on their source and composition: plant (cellulose based), animal (protein based) and mineral (such as asbestos). It is hypothesised that early humans started using animal fibres (the pelts of hunted pray) for protection from the cold somewhere between 200.000 and 30.000 B.C. [1]. Cultivation of plants to harvest their fibres begun much later as it required more coordination. Hemp is thought to be the most ancient cultivated source of fibres with documentation going back as far as 4500 B.C. in China [2]. The first evidence of woven and spun linen dates back to 3400 B.C. in Egypt suggesting that the cultivation of flax started some time before that [2]. The most ancient known use of cotton was found to date back to 3000 B.C. [2]. Chinese civilisation around 2640 B.C. was found to be the first to practice sericulture, i.e. growing silk worms to farm their silk for spinning.

In more recent years, starting from the industrial revolution, the utility of many more plant fibres was discovered. As will be discussed in section 2.2 the chemical composition and morphological structure of a fibre varies for every species of plant. The strengths and weaknesses of each species combined with the geographical availability has led to the ‘specialisation’ of fibres in different applications. The extraction process from the hosting plants has also been simplified thanks to the new machinery which was purposefully designed drastically reducing manual labour and consequentially increasing supply. Plant fibres experienced a commercial boom until the second world war, which is when the first synthetic fibre was developed by Wallace Carothers. In the 1930s it found a big place in the market as a unrivalled replacement for natural fibres for military purposing [3]. DuPont, for instance, replaced the need for importing plant fibres to make military parachutes and vests by replacing the plant fibres with lab-synthesised nylon. After the war, synthetic fibres would become a very common consumer product, competing with and replacing natural fibres to this day [3]. Since the year 2000 the production of synthetic fibres has more than doubled and is still increasing. 2018 saw a global production of 73.4 million metric tons of fibres of which just 6.8 million metric tons were plant sourced [4].

1.1.2. The history of composites

Composites is a term used for products that are composed of two or more materials. Early Egyptians and Mesopotamians (1500 B.C.) are the first to provide archaeological records of combinations of straw and mud utilised in the construction of habitations and storage rooms [5]. The first more impressive composite artefact is the Mongolian bow, which was used during Genghis Kahn's invasions (around 1200 A.D.). They were made by pressing wood and bone with animal glue and binding the product in birch bark. The result was a very powerful and accurate bow that could be shot from horseback [5].

In the early 1930s the first modern plastics such as polystyrene and polyester were being produced. The natural resins that were used up to that point were no match for these new materials, and began to be replaced by them. In 1935 Owens Corning created the first glass fibre, which when combined with the newly discovered plastics, would create incredibly light and strong materials. This discovery marked the beginning of the fibre reinforced polymer industry [5].

Warfare has always been a great motivator for the advancement of technology, and has brought modern FRPs from the lab into military use during the Second World War. With the end of WWII, producers had to find new applications for their innovative materials since the military demand had dropped. The first composite boat hull was in fact produced in 1946 [5]. In the same period, Brandt Goldsworthy (a.k.a. 'the father of composites') developed new composite products and manufacturing methods which are used to this day [5].

The late 90s saw composites being developed to their maturity. New and stronger synthetic resins/plastics and fibres were being invented, such as epoxy, HDPE, PP, carbon fibre and aramid, more commonly referred to as Kevlar, which is used in bullet-proof vests. Composites have become so strong that they can even replace steel in primary structures. It is hard to imagine something composites could not eventually achieve; in fact, modern research is currently focussing on nanotechnology, and composites are used in nanomaterials and nanostructures.

1.2. About the climate

As previously mentioned, our planet is facing an indisputable environmental decline since the industrial revolution has taken place in the late 1800s. The Intergovernmental Panel on Climate Change (IPCC) has published a report in 2018 containing all the current information regarding current state of the planet and related future risks. Figure 1.1 shows the different levels of threat that various human-supporting systems are already facing or going to face with a further temperature rise. The report also summarised the top five reasons for concern (RFC) as listed [6].

RFC1 - Unique and threatened systems:
'ecological and human systems that have restricted geographic ranges constrained by climate-related conditions and have high endemism or other distinctive properties. Examples include coral reefs, the Arctic and its indigenous people, mountain glaciers and biodiversity hotspots.'

RFC2 - Extreme weather events:
'risks/impacts to human health, livelihoods, assets and ecosystems from extreme weather events such as heat waves, heavy rain, drought and associated wildfires, and coastal flooding.'

RFC3 - Distribution of impacts:
'risks/impacts that disproportionately affect particular groups due to uneven distribution of physical climate change hazards, exposure or vulnerability.'

RFC4 - Global aggregate impacts:
'global monetary damage, global-scale degradation and loss of ecosystems and biodiversity.'

RFC5 - Large-scale singular events:
'are relatively large, abrupt and sometimes irreversible changes in systems that are caused by global warming. Examples include disintegration of the Greenland and Antarctic ice sheets.'

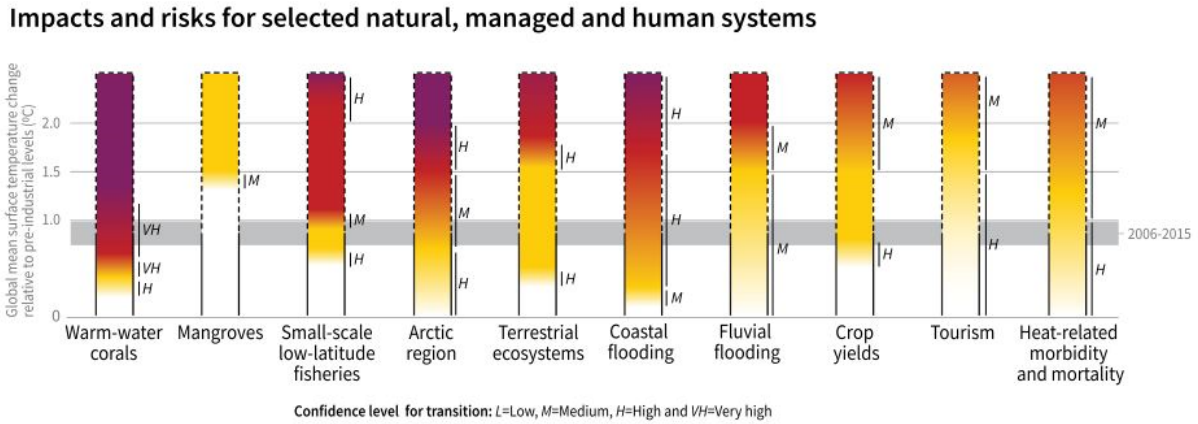

Figure 1.1: IPCC analysis of the impact of climate change on various human supporting systems [6]

Efforts to reduce emissions contributing to climate change are being made by many countries as agreed in the 2016 Paris agreement. The 2016 Paris agreement was of monumental importance and a first of its kind since it forced all countries to acknowledge climate change as a global threat and to set goals for all countries to achieve. Unfortunately the agreement is only a step in the right direction since the goals are non-binding and not remotely sufficient when it comes to meeting the goal set: arresting the progression of climate change at no more that 1.5°C. In light of this, the sustainability of material sourcing, product manufacturing and disposal, has become a very important topic to focus on regardless of the field of expertise. Climate experts are calling for intimidate action in order to prevent crossing the 'point of no return', which is the name given to the level of emissions after which the planet will continue heating even if all emissions would stop, as a consequence of complex climatic feedback loops. After this point, the climate crises can only be mitigated instead of prevented.

While in use, composites actively contribute in the decrease of emissions in the transportation sector since lighter vehicles require less fuel to travel a specific distance. Their synthesis and disposal however are often responsible for (either or both) environmental pollution and greenhouse gas emissions. As they decay, plastics release 'micro-plastics' which can be consumed by micro-organisms or small animals. Micro-plastics are an additional reason for concern since they can eventually work their way up to our own diet through the food chain at dangerous concentrations [7].

1.3. Problem statement

In recent years more research has been done aimed at finding alternatives to synthetic composites in an attempt towards reducing anthropogenic emissions and pollution. Replacing the fibre and/or the matrix with a sustainable and biodegradable material would decrease both the energy invested in creating the composite as well as the waste produced after the product has reached the end of its life-cycle. Natural and synthetic biodegradable materials however are almost always outperformed by plastics, making them less attractive for structural applications. Plant fibres and bio-polymers are still being developed and are showing to have the potential of replacing synthetic materials in non-structual applications, single-use items, sports equipment and can even be adopted in designer applications. Since adhesion is a crucial point of improvement for the performance of plant fibre composites and their applicability towards a larger market range, this thesis is focused on the effects of alkalisation on the adhesive properties of flax fibres.

2

Background knowledge

In this chapter the background information used to formulate the research questions is presented. The research can be divided into four topics before the concluding research questions are presented. First of all, the existing literature on the sourcing of plant fibres is presented, followed by a section dedicated to their morphology, chemical composition and mechanical properties. One section is dedicated to the existing literature on alkalisation of flax fibres, and one to testing methods quantifying the interfacial properties of fibres. Review papers give a good overview of the recent publications regarding plant fibres (especially flax) for composite applications (see sources [8–18]).

2.1. Plant fibres: what they made of and where they come from

Plant fibres are composed of cellulose, hemicellulose, pectin, lignin and waxes in different proportions depending on the species. Plant fibres can be divided into bast, leaf and seed fibres. Bast fibres (bamboo, begasse, flax, hemp, jute, kenaf and raime) are obtained from the plant stem and are made up of overlapping cells. On average, they retain the best mechanical properties out of the three plant fibre sub-categories. Leaf fibres (abaca, banana, henequen, phormium, pineapple and sisal) are obtained from the leaf's fibrovascular system and can have a wider range of mechanical properties, sometimes competing with some bast fibres. Seed fibres tend to be shorter, coarser and more brittle (coir, cotton and kapok) [8, 9]. The method by which the fibres are extracted from the part of the plant that hosts them affects their mechanical properties, making it a relevant piece of background knowledge.

2.1.1. Fibre extraction methods

Plant fibres can be extracted from different parts of various species of plants. Separation[1] of the fibres from their biological structures is usually either done through decortication or through retting. Decortication consists in removing the fibres from the plant by breaking and washing off the rest of the plant. The wet fibres are then dried, brushed and graded. This process is easier for bast fibres as the woody stems is simply beaten/shaken off. This process requires energy to actuate the mechanical vibrations [19]. The waste could be used for biomass or fertilizer for other plants. Retting consists in exposing the stems to moisture for a prolonged period of time to facilitate the removal of the fibre from the woody tissue by partial and controlled rotting. Retting can be performed in three different ways depending on the wished speed and cost of the process. A quick overview of the three different methods is given below:

- **Water retting** is the most used process and consists in submerging bundles of stalks in water. This can either be done in stagnant/slow moving water (two to four weeks) or in tanks (a few days). In the latter the toxic waste water needs to be processed before it can be introduced back into the environment. The advantage however is that the fibres have more controlled and consistent quality. Once processed, the water can be used as liquid fertilizer because it is rich in plant minerals. Immersion time is critical: *under-retting* makes separation difficult, *over-retting* deteriorates the fibres. *Double retting* is a more advanced technique that consists in first under-retting the bundles to then dry them for several months and then retting them a second time yielding higher quality fibres [19, 20].
- **Dew retting** is the most popular method in Europe and other places with less available bodies of water. It is most effective in locations with warm daytime temperatures and heavy night time dews. The stems are left in the field for controlled rotting for two to six weeks depending on the atmospheric conditions. The fibres obtained are darker, coarser and have a lower quality when

[1] In literature the Duralin treatment repeatedly shows up as a very efficient extraction method. Puglia et al. even claim it can completely replace the most common form retting [11]. When no current information could be found about having this procedure done, it was discovered that the company doing this process has gone out of business by finding the contact information of an old employee. The Duralin treatment is therefore no longer available.

compared to fibres separated through water retting. It is very cheap and not labour intensive when compared to water retting [9, 19, 21].

- **Chemical retting** consists in the immersion of dried plants in a tank with the addition of various chemicals to separate the fibres in just a few hours. It is more expensive and the usage of chemicals for the process results in large quantities of chemical waste water.

2.1.2. Fibre treatments

When the fibres have been separated from their biological structure some form of woody debris will still be stuck to the fibres. The removal of the woody debris is done by first drying the fibres, breaking the woody parts by passing the fibres through fluted rolls and then removing the crumbled debris by scutching. Scutching consists in beating the fibres with blunt wooden or metal blades [19]. Seed fibres, which are short and 'fluffy' are spun into yarn, while longer fibres like bast and leaf require to be aligned before they can be spun into yarn. Alignment of long fibres is done through hackling, which consists in beating them onto a set of pins with increasingly smaller spacing. A final purification step can be taken after either scutching or hackling: carding. Carding consists on passing the fibres on pinned rolls that increase the fibre alignment even further. Carding also reduces the lengths of the fibres by breaking them at weak points. Carded fibres have more consistent properties (smaller variance) due to the decrease in weak points. Once any additional purification and refining treatments have been done, the fibres can be spun into yarn.

2.1.3. Fibre selection for structural applications

Data from various papers and review all agree that, with the exception of some leaf fibres, bast fibres in general are the most suitable for commercial and structural applications due to their lower costs, better mechanical properties and chemical composition. Trade-off criteria to determine which plant fibre have the biggest potential to be commercially viable for structural application must consider both fibre mechanical properties and cost of the raw fibre. Dittenber et al. created a bar chart showing the cost per metre of the amount of fibres required to withstand a load of 100kN and compared it with glass fibre. From this chart only (bast fibre) jute, kenaf, bamboo, lower-cost flax or hemp and (leaf fibre) sisal could potentially compete with glass fibre on the market in terms of cost and mechanical properties [8]. This first selection suggests that bast fibres, with the addition the leaf fibre sisal, are potentially better candidates for marketable structural applications and were therefore worth further investigation.

2.2. Properties of bast fibres

Knowing the biological composition of bast fibres is essential to understanding how they correlate to the mechanical properties. The mechanical properties and failure mechanisms are governed by the microscopic structure (morphology) and chemical composition of the fibres. As previously mentioned, bast fibres are obtained from the stem, which in general is composed of three main parts: the bark which encloses the structure, the fibres that give it strength and a core.

2.2.1. Morphology

The macroscopic structure (from outward) of a plant stem is composed of: bark, phloem, xylem, and a central void. The bark of the stem of the plant exists to protect the internal structures of the plant and retain the moisture, just like the human skin. Underneath this protective layer the elementary fibres bundles are found, in what is called the phloem. They give the plant its stiffness and strength. Deeper inside, the systems responsible for the transportation of nutrients and water to the rest of the plant can be found (Figure 2.1) [22].

The phloem is the part of the stem that contains the elementary fibres of interest, which are bound together into bundles by a substance known as the middle lamella which essentially is composed of pectin (Figure 2.2) [22]. An elementary fibre bundle in general is a collection of 10 to 40 elementary fibres and the average diameter of a single (flax) fibre is 12 to 20 μm [10, 23]. Different plants have different fibre diameter ranges.

Taking a closer look at an elementary fibre within a bundle, it is possible to see that they are made up of cells (Figure 2.3). The most outer part is made up by the primary cell wall and is approximately 0.2 μm thick [10]. This thin cell wall's purpose is to protect the thicker secondary cell wall which is responsible for the fibres strength. Within the secondary cell a concentric void is found which is called the lumen, which is responsible for the water absorption of the plant. The secondary cell is composed of the S1, S2 and S3 layers. The S1 layer, like the primary layer, is resistant to swelling caused by water and acetic

acid. The S2 layer, which accounts for 70-80% of the mass of the elementary fibre [22], is responsible for the strength of the fibres. The orientation of the fibrils with respect to the fibre axis (micro-fibril angle, MFA) affects the mechanical properties. In general, a low micro-fibril angle results in high stiffness and tensile properties, whereas a large angle results in higher ductility [24]. The micro-fibrils in the S3 layer are oriented at a greater MFA making it a layer effective in resisting the hydrostatic pressures exerted by the lumen [9].

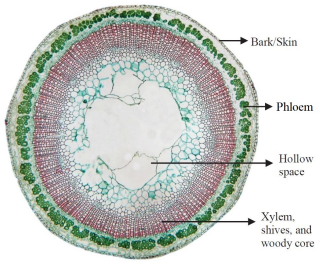

Figure 2.1: Flax stem cross-section [22]

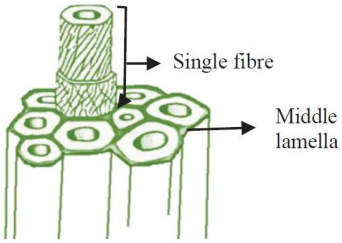

Figure 2.2: Elementary fibre bundle [22]

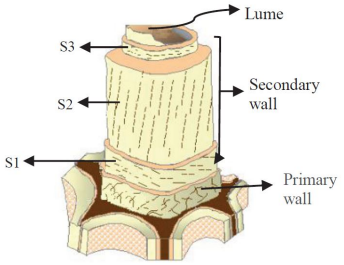

Figure 2.3: Elementary fibre [22]

2.2.2. Mechanical properties and chemical composition of bast fibres

The mechanical properties and chemical composition of a plant fibre are highly dependant on how, when and where they were grown, as well as the species, harvesting and fibre-extraction techniques used. Imperfections in the fibres and weak points can originate from damage (kink-bands) and natural imperfection, making it very hard to have consistent mechanical properties throughout the length of the fibres.

In general, cellulose is the dominant compound in bast fibres, followed by hemicellulose and lignin. Pectin is present alongside small amounts of wax and fat in the S2 layer make up only 1 to 4% of the fibre [22]. Table 2.1 compiles information from literature regarding the relevant mechanical properties and chemical composition of the five most cost effective per 100kN load plant fibres as determined by Dittenber et al. [8].

Table 2.1: Trade-off properties for fibre selection for structural applications [10, 22, 23]

Fibre	Unit	Flax	Hemp	Jute	Kenaf	Sisal
MFA	deg	10	6	8	–	20
Diameter	μm	12-20	15-30	14-20	14-33	–
Tensile strength	MPa	500-900	350-800	200-450	–	100-850
Elongation	%	1.5-4.0	1.6-4.0	1.2-3.0	1.7-2.1	2.9-6.8
E-Modulus	GPa	50-70	30-60	20-55	4.3-60	9-22
Cellulose	wt%	65-85	60-77	45-63	45-57	50-64
Hemicellulose	wt%	10-18	10-17	12-15	21.5	10-14.2
Lignin	wt%	1-4	3-10	12-25	8-13	10
Pectin	wt%	1-3	1-3	0.2-3.0	3-5	1

Cellulose, a strong crystalline linear polymer composed of carbon, hydrogen and oxygen, is the main structural component in plant fibres. It is a polysaccharide which is prone to degradation when it undergoes oxidation, hydrolysis or dehydration [11, 25]. Hemicellulose, which is highly hydrophilic [22] because it is mainly responsible for moisture absorption [11], is a low strength amorphous polymer which is often a copolymer of glucose, mannose, gluconic acid, arabinose and xylose. It is also easily hydrolysed by dilute acids or bases. The removal of hemicellulose and lignin, which together form an encasing matrix for the cellulose [22], is essential to improve the strength of the composite since bonding directly with cellulose creates a stronger bond [8, 25]. Lignin in an aromatic structure that forms during the lignification process of the plant and it provides it with mechanical stability. The process of lignification is irreversible and occurs by the removal of water from the sugars such as xylose. Lignin protects the plant from external attacks such as micro-organisms or anaerobic processes. Pectin mainly acts as a binder in elementary fibre bundles and is present in the lowest quantities in plants [25].

Flax and hemp are the bast fibres that are most suitable for structural applications due to their superior moduli and tensile strengths. While flax is observed to have a lower MFA in general, its higher cellulose

composition gives it the superior modulus. Flax is also more commonly used as a technical fibre in both research and non-structural applications. The most recurring source on flax fibres is the work performed by Baley and Bourmaud, wherein the relationships between different elementary flax fibre properties are examined [26]. Most notably, a decreasing fibre strength was observed with an increase in fibre diameter, while a higher tensile strength was associated with a higher tensile modulus. This suggests that the fibre efficiency decreases with an increasing diameter. After testing 2954 French elementary fibres of 12 varieties, they found that on average, the diameter, modulus, tensile strength and elongation of the fibre respectively are 16.8$\pm$2.7μm, 52.5$\pm$8.6 GPa, 945$\pm$200 MPa and 2.07$\pm$0.45%. Lefeuvre et al. have gone as far as investigating the variation in fibre properties over the height of the flax fibre plant [27].

2.2.3. Closing remarks on plant fibres

The main issues with plant fibre composites are fire resistance, moisture content and absorption, limited processing temperatures, fibre agglomeration and the formation of hydrogen bonds. Furthermore, the mechanical properties of plant fibres are subject to scatter due to naturally occurring defects in their structure and inconsistent fibre thickness. It is agreed that the largest point of improvement was found to be the incompatibility between the hydrophilic fibres and the hydrophobic matrix, leading to poor wettability and consequentially low interfacial properties [8]. Up to this day, more research is required aimed at improving the interfacial properties as they have been found to significantly affect the overall properties of plant fibre composites. Experimental research has been carried out on how to improve the bonding between the two materials at the interface by using both physical and chemical treatments. In the following list the most important definitions from the section are recapitulated:

An elementary fibre
is the most basic fibre with an average diameter of 12-20 μm

A fibre bundle
consists of, on average 10 to 40 elementary fibres bound to together in the middle lamella, which is mainly composed of pectin.

A technical fibre
is a yarn of aligned and spun elementary fibre bundles.

Cellulose
is the main structural component of the plant and is sensitive to degradation by oxidation, hydrolysis or dehydration.

Hemicellulose
is responsible for moisture absorption (hydrophilic) and is not a structural part of the fibre. Removal of this compound is key to improving bonding with a polymer matrix and can easily be achieved by hydrolysis in dilute acids or bases.

2.3. Treatment of flax fibres

This section focusses on the effects treatments have on flax fibres. Treatments can be divided as physical or chemical. A physical treatment consists in using non-chemical methods to alter the structural composition of fibres aimed at increasing the surface energy which will improve wetting. A chemical treatment consists in exposing the fibres to a chemical solution with the objective of altering the chemical composition and/or the surface topography of the fibres. The objective of chemical treatment is removing detrimental compounds and improving the fibre surface for bonding.

2.3.1. Effects of physical fibre-treatments on flax-epoxy composites

This section mainly focusses on the work performed by Isabel van de Weyenberg at the Technical University of Eindhoven in order to obtain her doctoral degree. Her work is the most extensive when it comes to investigating the effects of physical fibre treatments on the properties of UD flax-epoxy composites. She has investigated the effects of the fibre refining processes on 12 different grades of flax fibres to determine the which combination is most suitable for composite applications. The grades of the fibres were determined by the degree of retting (barely retted or green, half-retted or normally retted) and whether they had been scutched (long flax), hackled (long flax), scutched and carded (tow) or hackled

and carded (tow) [23].

Van de Weyenberg observed that plant fibre production is tailored to the textile industry. Purification, refining, bleaching and spinning are costly additional processes that do not add to the value of fibres when used for composite applications. Van de Weyenberg argues that flax fibre composites would be much more cost effective if fibre-processing halted at hackling or scutching. The use of short chopped fibres would decrease costs even further. The methods by which fibres are extracted (cutting, retting, scutching, hackling, carding and spinning into yarn) has been explained in section 2.1. Each step increases the cost per kilogram of the fibres to almost an exponential degree [23].

Effect on the elementary fibres

From testing the elementary fibres she found that when it comes to long flax, green fibres do indeed yield a lower strength and higher fineness of the fibre (more coarse). This can be attributed to the higher amount of removable non-structural chemical compounds in under-retted long flax fibres. Van de Weyenberg found no proof that half-retted long fibres are more brittle than green long fibres. When the results of normally retted scutched or hackled tow were compared, she found clear evidence that higher fibre strength and lower variability was achieved with the hackled tow variant due a lower amount of impurities leading to finer fibres [23].

On the topic of elementary fibres, final remarks were made on de dependency between the frequency of kink-bands in the fibres and the fluctuation of the results. Kink-bands are essentially regions of the fibre that have been damaged during the processing. Van de Weyenberg argues that hackling after scutching may be favourable to simply scutching since it yields a lower variability of the results despite it being associated with a lower fibre average strength. Lower average strength and lower variability are due to the high frequency of kink bands, making the mechanical properties of the fibre more predictable by ‘certainty of damage’ [23].

Effect on the tensile strength and modulus of UD composites

Van de Weyenberg found that when grouping the tests by degree of retting, full-retting yielded the best results with little variation for any subsequent physical fibre treatments. When grouping the tests by the kind of physical treatment they had undergone, she found that hackling yielded good properties with small increments associated with a superior degree of retting [23]. Composite properties are associated with the amount of impurities in the fibres. Retting de-polymerises weaker pectin and hemicellulose, while hackling makes the fibres more homogenous, increases their fineness and removes impurities. Van de Weyenberg found that the degree of retting has the biggest effect on the longitudinal composite strength, concluding that a complete retting process yields the best properties. The length of the fibres and whether they had only been scutched, or scutched and hackled did not show significant changes in the properties. When comparing the results of the 12 grades of fibre with regards to the longitudinal modulus, the long fibres outperform the carded fibres. While the degree of retting had no significant effect on the modulus, hackled fibres did perform better than scutched in both mean and variance due to the increased fineness and purity of the fibres.

Issues with plant fibres

The study on the effects of physical fibre treatments on flax fibre composites performed by Van de Weyenberg was found to be the most complete and extensive piece of literature to date. Her findings reinforce, with significant evidence, the hypothesis that the poor adhesive properties between the fibre and the matrix caused by impurities in the fibres is the element to most likely lead to the failure of the material. A second important element leading to failure is the increased probability of fibre damage in lesser processed fibres, which are responsible for crack nucleation, which when propagated lead to failure due to high local stress concentrations. Van de Weyenberg’s objective was to determine which physical treatment combination led to the best ration between material properties and cost. She concluded that scutched and carded tow would yield the most cost effective flax fibre composite in terms of performance over cost ratio. In the next section, methods to improve the adhesive properties between the fibre and the matrix are examined.

2.3.2. Effects of chemical fibre treatments

Fibre modification through chemical treatment consists in modifying the surface, structure and/or the chemical composition of the fibre by exposing it to a chemical substance. It was previously determined that hemicellulose can be hydrolysed by exposing it to a diluted acidic or basic solution. In most cases, weak solutions of NaOH or KOH are used for this purpose. The aim of the treatment is to increase

the interfacial shear strength of the flax fibre composite. A wide range of chemical treatments can be applied. The literature reviews mentioned so far describe a wide range of options, and often conclude that silanes often yield the best results [10], while alkalisation (with NaOH or KOH) is the easiest to carry out [8, 12, 14, 18].

Alkalisation of flax fibres with dilute NaOH solution

Alkalisation is one of the most popular surface treatments to improve the interfacial properties of plant fibre composites. This section focusses on the effects the treatment has on the fibres and consequentially the composites as can be found in literature.

The adhesive properties between the two materials can be improved through three mechanisms. First of all, the hydrolysis of hemicellulose decreases the moisture absorption capacity of the fibres which essentially makes them less hydrophilic. Secondly, fibrillation increases the surface roughness and bonding surface area. Finally, the hydroxyl groups in the cellulose are attacked (as shown in eq. 2.3.2), which contributes to decreasing the hydrophilicity of the fibres [8, 12, 18, 28]. Alkalisation with sodium hydroxide (NaOH) occurs as follows:

$$\text{Cell} - \text{OH} + \text{NaOH} \rightarrow \text{Cell} - \text{O}^{-}\text{Na}^{+} + \text{H}_2\text{O} + \text{impurities [18].}$$

The removal of hemicellulose and other non-structural compounds creates new available space within the fibre, which is filled by the fibrils adjusting their orientation into the tensile direction. The removal of the non-structural compounds also decreases the density of the fibre and increases the collective crystallinity of the fibre as its percentage composition with respect to cellulose increases. The elastic modulus of the fibre is expected to increase with the increased molecular orientation brought on by the reduction in the MFA as a consequence of alkalisation [18, 28, 29].

The main variables that affect the strength of the treatment are the temperature, solution concentration and the amount of time the fibres are exposed to the solution. Over-treatment by over-exposure or excessive concentration degrades the fibre, resulting in a loss of mechanical properties because of delignification and depolymerisation of the cellulose [8, 18]. Over-treatment can be mitigated by first soaking the fibres in distilled water after the treatment, then subjecting them to a slightly acidic solution to neutralise the lingering treatment solution absorbed by the hydrophilic fibres, and finally rinsing them in distilled water again [8, 30]. Alternatively, thoroughly rinsing the treated fibres under running distilled water is also sufficient [23]. Ideally, treatment takes place in an automated system before the fibres are rolled on a drum. Figure 2.4 shows an example of how the treatment can be done on an industrial level to yield a drum of dry fibres (left) and a drum of pre-impregnated fibres.

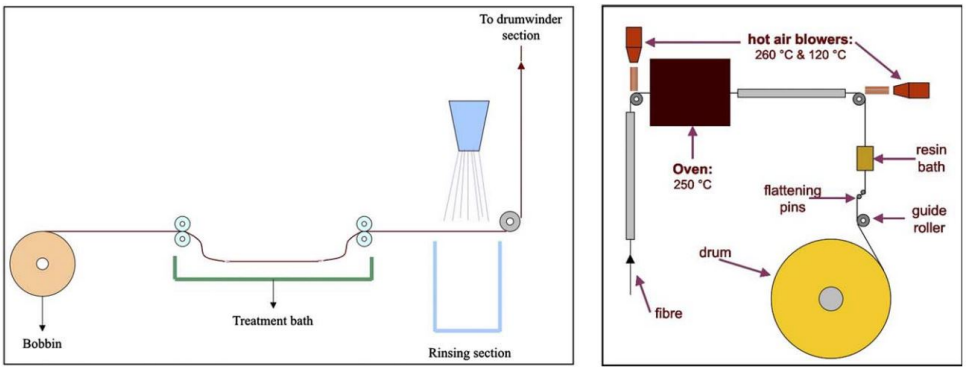

Figure 2.4: Surface treated flax yarn - Fully continuous method [31]

Effect on technical fibre properties

Since alkalisation affects both the chemistry of the fibre as well as its topography, a literature study has also been done regarding the change of their tensile properties after testing. Symington et al. have performed tensile tests on (presumably, due to large gauge length) technical fibres that have been exposed to a 10, 20 and 30 minute 30% NaOH surface treatment [28]. Their tensile tests were performed as close as possible to the ASTM D 3822-01 international standards. They found that both the failure strain and tensile strength decrease with an increase in exposure, while the modulus only decreases with the 30 minute exposure sample. They suggest that maximal fibre properties are achieved by subjecting the fibres to treatments with exposure times inferior to 10 minutes [28, 29].

Effect on flax fibre composite properties
Van de Weyenberg has conducted an extensive study on the subject of alkalisation treatment of flax fibres [23, 31, 32]. In her research she investigated the importance of fibre-processing with regards to the flax-epoxy composite as well as the effects of different levels and methods of alkalisation treatment. She concluded that the best flax-epoxy composites are obtained through treating the fibres with a 3% alkali solution and subsequently impregnating them with acetone diluted epoxy. She claimed that an increase of 40 and 60% is respectively possible in the longitudinal bending strength and stiffness properties, while the transverse bending and stiffness properties can increase by to 200 and 500% respectively.

A study by George et al. utilised non-woven mats of flax fibres and submerged them in a 1% NaOH solution for one hour. A low concentration HCl solution was used to neutralise the sodium hydroxide and the fibres were then dried for one hour at 105 °C. After testing the flax/epoxy composite increments of the tensile strength, tensile modulus and impact strength of 60, 9 and 13% respectively were reported [33].

A study by Prasad et al. showed that after submerging coir fibres for 72 to 96 hours in 5% NaOH yielded a 15% improvement in mechanical properties of the fibre occurred, while the mechanical properties of the composite improved up to 40%. When the treatment time was extended the fibred began to degrade, and the degradation process was found to be faster when the alkali solution was replenished every 24 hours. Through longitudinal ultrasonic velocity and sound attenuation measurements the increment in composite mechanical properties was attributed to improved bonding and decreased fibre segregation after the alkalisation process [30]. It is important to note that the chemical composition is of coir is very different to flax which results in different optimal treatment times.

2.4. Single fibre tests for IFSS determination

Micro-mechanical shear tests on individual fibres are, in theory, the best methodology to determine the interfacial interaction between a fibre and the polymer matrix. Unfortunately these tests are not yet standardised. It is however possible to find literature on the methodologies adhered by various research groups. The variability in methodology leads to variations in the interpretations of the results obtained by the different research groups. The most popularly suggested methodologies to determine the change in interfacial properties are the fibre pull-out test, the micro-drop test and the single fibre fragmentation test (SFFT). In all three cases, sample preparation can be difficult due to the minute size of the samples. The numerical interpretation of the results after testing is also subject to discord and discussion [34]. The boundary conditions of the single embedded fibre are different than they would be in a consolidated laminate [35].

Micro-bond test
The interfacial shear strength over the length of the fibre can be theoretically described by the Cox equation (eq. 2.1) where σ_{fu}, r, l_c, and τ_y respectively describe the tensile strength, radius and critical length of the fibre and the IFSS of the interface under the assumption of fibre homogeneity and fibre governed modulus [36]. However, fibre homogeneity in fibres is impossible. Khalil et al. proposed a variation on the Cox equation by using the micro-bond test to determine the IFSS of plant fibre composites (eq. 2.2). τ, d, L, F_d respectively describe the IFSS, fibre diameter, micro-droplet length and maximum debonding force [36]. The maximum embedded length is usually small making the test very hard to set up and making the data subject to scatter. Further complication arise from the effect of matrix shrinkage affecting the pull-out force and friction coefficients in the stick-slip mechanisms [37].

$$\frac{\sigma_{fu}}{\tau_y} = \frac{2l_c}{r} \tag{2.1}$$

$$\tau = \frac{F_d}{\pi d L} \tag{2.2}$$

Most of the literature on micro-mechanics presents large scatter in the results [38] and is focussed on thermoset carbon/glass fibre composites [39], which are not subject to the same degree of scatter and fibre inhomogeneity when it comes to the mechanical properties of plant fibres [15, 36].

Fibre pull-out test
The fibre pull-out test consists in embedding a section of the fibre in a polymer matrix and evaluating the tensile force required to pull the fibre free of the matrix that is encasing it. This test requires the ultimate tensile stress of the fibre to be superior to the tensile force required to pull the fibre free of the matrix.

Two variation of this test exist: the first (Type-I) consists in clamping the matrix at the stress-free end and pulling on the fibre from the other side, while the second (Type-II) variant consists in supporting the matrix on the same side as where the fibre is to be pulled out of. Sørensen et al. describe a simplified lag-shear model for Type-II pull-out based on the debonding energy and the constant sliding shear stress that includes the effect of residual stresses. They however exclude the Poisson's effects which allow for the model to be 1-dimensional. They also claim that the model is closely related to the ones that can be applied for Type-I pull-out and SFFT [34]. The model consists of three stages: "debonding and sliding phase, the load drop at maximum fibre stress and the sliding and pull-out phase to complete pulling-out of the fibre" [34]. The fibre pull-out test is most suitable for surface treatment studies with high ultimate tensile strength fibres and low/medium IFSS, which is not the case when looking at plant fibres [37].

Single fibre fragmentation test
Van de Weyenberg suggests that single fibre fragmentation might be suitable for plant fibres [23]. Sørensoen et al. [34] provide an in-depth numerical analysis of the interface interaction in the pull-out test and the single fibre fragmentation test, while Feih et al. have attempted the experimental analysis of SFFT with glass fibre [40].

The SFFT consists in subjecting a polymer matrix dog-bone encasing a single fibre to a tensile test while observing it under crossed polarised light to view the samples photoelastic response. The tensile loads applied on the matrix are transferred to the fibre by shear stress, meaning that the larger the disparity in Young's modulus and failure strain, the better the test will work. Where the critical stress is reached, the fibre will fragment. The stress concentrations and failures are visible under cross-polarised light (thanks to photoelasticity) in the form of birefringence patterns. Shear loading implies a minimum fibre length exists for it to be able to fragment. The driving requirement for the test to be used is for the fibre to have a failure strain inferior than that of matrix, else the matrix will fail before the fibre can fully fragment. At fragmentation saturation, the interfacial shear strength can be evaluated from the lengths of the fragmented fibres and the fragmentation frequency [34, 40, 41]. It has only recently been theorised that characterisation in terms of frictional stress and debonding energy might be more applicable since fibre failure takes place progressively [34]. Since no ASTM or ISO standards currently exist for the single fibre fragmentation test, but guidelines and points of improvement of researchers that have attempted it exist alongside the mathematical models to evaluate the interfacial properties [40, 41]. When it comes to synthetic fibres, the results obtained through this method are reasonably consistent and repeatable as long as the set-up procedure is unchanged. Results obtained from different laboratories however show variations in their findings when compared [40].

2.5. Conclusions from the literature study

In this section the findings from the literature study are summarized in a way that they can lead up to research questions that will guide the thesis.

The main difference between seed, leaf and bast fibres were explained as well as the methods by which the fibres are extracted from their woody hosts. Several physical treatments exist in the textile industry to increase the quality of the fibres by removing impurities, kink-bands and increasing the fineness. Since the processing of plant fibres is tailored around the demands of the textile industry, it is possible that some of the treatments are not suited for composite applications. This section concludes that bast fibres are in general most suited for composite applications.

Plant technical fibres are composed of inter-spun bundles of elementary fibres, elementary fibre bundles are composed of groups of 10-40 elementary fibres, bound together by a substance called pectin. Cellulose responsible for the mechanical properties of the fibre, while hemicellulose is responsible for water absorption. The latter can be hydrolysed with dilute acids and bases resulting in a decreased ability to absorb water. Flax was as the main fibre candidate because of its favourable properties, increased availability and available literature investigating its use in composites.

Van de Weyenberg investigated the effects of the purification steps flax fibres are subjected to in preparation for the textile industry on their performance as a flax - epoxy composite. She concludes that for structural applications, any steps after scutching and/or hackling would be not worth financial cost. Hackling after a fully retted procedure yields the best mechanical properties for flax fibre composites. The most common form of chemical treatment aimed at hydrolysing hemicellulose is alkalisation with sodium hydroxide. Treatments above 10 minutes potentially deter the tensile properties of the fibres, while in flax-epoxy composites a mild treatment (2-3% for less than 30 minutes) was found to have a beneficial effect on the tensile and transverse properties of the composite. The literature covered in this section allows for the formulation of the first guiding research question:

What are the effects of sodium hydroxide treatment concentration and exposure time on the tensile properties of technical flax fibres?

Improving the adhesion between flax fibres and epoxy is thought to be crucial to increase the application of plant fibres in more sectors. Adhesion can be measured by quantifying the interfacial shear strength between the two materials, and three tests involving synthetic fibres are commonly reported for this purpose: the micro-bond test, pull-out test and single fibre fragmentation test. Out of the three, SFFT seems to be the most suitable for plant fibres, since their tensile strength is lower than that of synthetic fibres. The SFFT does not have a standardised methodology, therefore the work done by previous authors with synthetic fibres is to be used as a guideline. Determining the feasibility of this test in combination with flax fibres is the guideline for the second research question:

What are the effects of sodium hydroxide treatment concentration and exposure time on the adhesive properties of elementary flax fibre bundles in a single fibre fragmentation test?

3
Methodology

This chapter will focus on the methodology developed in this research process such that the experiments may be reproduced as consistently as possible. The methodology in preparation for the experimental part of the project can be divided in into three main parts:

1. Technical fibre preparation, characterisation and verification
2. Dog-bone production and characterisation
3. Single fibre fragmentation test instrumentation and execution

3.1. Technical fibre preparation, characterisation and verification

This section provides a detailed account of the methodology that has been developed to apply the flax technical fibre surface treatment with NaOH, as well as the determination and verification of their tensile properties. The flax fibres used have been grown in France and have been delivered by the Swiss based company Bcomp. The company is specialised in the production of flax fibre weaves that can be used to reinforce polymers for structual applications. The most common treatment methodologies have been explained by Figure 2.4, however these automated treatments take place before the fibres are woven into weave. Since Bcomp delivers only untreated fibres an impromptu setup had to be devised in order to apply a controlled surface treatment on the fibres.

3.1.1. Flax fibre NaOH surface treatment

The main purpose of alkalisation is the hydrolysation of the hydrophilic hemicellulose with the objective to increase the compatibility with epoxy. Repeatability of the treatment has been assured by maintaining a constant proportion between distilled water and the total length of exposed fibres while only varying the quantity in weight of soluble NaOH to control the concentrations of the solutions. For each set the following equipment has been used alongside the relevant safety equipment:

1. Glass container
2. Volumetric flask (500ml): distilled water
3. Balance
4. Soluble NaOH
5. Paper cups for weighing
6. Magnetic stirrer
7. 20×1m technical flax fibre

Solution preparation

The concentration of the solution was determined by multiplying the weight of the water (500g) by the wished achieved NaOH (weight) percentage: 1% NaOH = 5g NaOH + 500g H_2O. Weighing the compound is time sensitive since NaOH readily absorbs moisture from the air which manifests in the form of pellet glossing. Using a magnetic stirrer in combination with a round glass container favourably affects both the dissolution time and solution homogeneity. The reaction between NaOH and H_2O is exothermic due to the creation of Na^+ and OH^- ions in the solution, therefore cooling time is required to allow it to return to room temperature.

Fibre surface treatment

Flax fibres are delivered by the manufacturer on a 1 metre wide roll, providing technical fibres of equal lengths. Handling of the fibres should be done while wearing latex gloves to prevent contamination through skin contact. Bundles of 20 technical fibres were made by tying them together at one extremity with a plain knot.

The fibres are submerged in the room temperature NaOH solution for a predetermined period of time (Table 3.1), at the end of which they are carefully and thoroughly rinsed with running distilled water to

remove any alkali residue that might further affect the surface of the fibres. Before being introduced into the oven to dry overnight at 50°C the fibre bundles are left to hang and drip for 45 minutes. Figure 3.1 shows what the fibres looked like during the treatment. In the left container a lower concentration is used than in the container on the right. It is observed that the solution with the higher concentration obtains a darker shade of green, and that the fibres in the container have become more swollen and fuzzed. The darker water is probably due to the dissolving of organic matter in the fibre and the fibre fuzziness is probably due to fibrillation and fibre shrinkage.

The test-matrix was devised such that the effect of an increasing NaOH concentration (1 to 5%) could be tracked over a constant exposure time (45 min) as well as investigating the extremes of the test-matrix. The lower extreme of higher exposure time at low concentration (1% and 120 min), the high concentration (10+% and from 45 to 120 min) as well as the progressing effect increasing exposure time at a concentration that was concluded to be effective from literature (5% for 30 to 120 min). 20 technical fibres are treated in every batch, since the tensile test is repeated 20 times. Additionally to the test-matrix, there is a controlled group of fibres. These are untreated and come straight from the roll.

Table 3.1: Test-matrix – Investigated exposure times and NaOH concentrations for the tensile test

Treatment	30 min	45 min	60 min	90 min	120 min
0% (H_2O)		x			
1%		x			x
2%		x			
3%		x			
4%		x			
5%	x	x	x	x	x
10+%		x	x	x	x

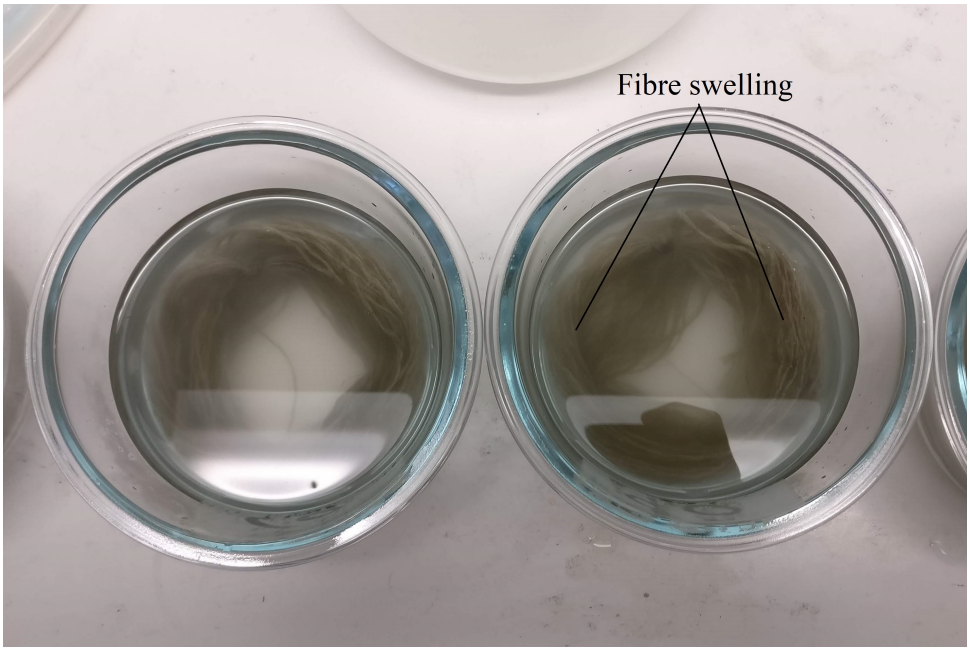

Figure 3.1: Alkalisation treatment of flax fibres. Left: lower concentration; Right: higher concentration showing swelling and fuzzing of the fibre

3.1.2. Flax fibre characterisation and verification

In the literature section it was established that plant fibres are subject to a high degree of scatter in all of their mechanical and chemical properties due to their nature. Bcomp has delivered a strand of technical fibres which they claim is capable of achieving consistent results when they are infused for composite applications. A technical sheet containing information about the technical fibres states that the E-modulus and the tensile strength respectively equal 60GPa and 800MPa [42]. It is also stated that the fibres are grown in France and Belgium, making them relatively locally sourced. The aim of the below described tests is to determine the effects of the surface treatments on the mechanical properties of the fibres while verifying the material properties stated by Bcomp. The D 3822 ASTM international guidelines for testing single fibres is focussed on synthetic fibres, and therefore are not in detail applicable to the testing of plant fibres, which are subject to significantly more scatter. Nevertheless the ASTM guideline has been used for the estimation of the tensile properties of flax fibre.

Technical fibre tensile test

In this section the processing of the data obtained by the tests is explained, with the control group fibre data-set (untreated, as received) as an example. The tensile tests of the technical flax fibres are performed with the Zwick tensile test machine, and data is digitally collected in the form of load measured in Newtons by the load-cell and the recorded displacement in millimetres of the extensometer as a consequence of the strain controlled increments. Data recording begins once the pre-tensioning load of 5N is reached, with the first recording of measured displacement and force being noted as L_0 and F_0. Each fibre data-set group is repeated 20 times as suggested by the ASTM international standards. Technical fibre tensile tests are performed with a 20kN Zwick tensile machine mounted with suitable coiled clamps and an extensometer with a 50mm gauge length. Figure 3.2 shows the setup adopted throughout the strain controlled tests. To prevent slipping of the fibres on the coil while the test is running a pre-tensioning force of 5N is applied at a strain rate of 50 mm/min. The extensometer begins recording data until fibre failure once the 5N pre-tensioning load is reached maintaining the 50mm/min strain rate. Data is recorded by the software as the force measured by the load cell in Newtons and the elongation measured by the extensometer in millimetres.

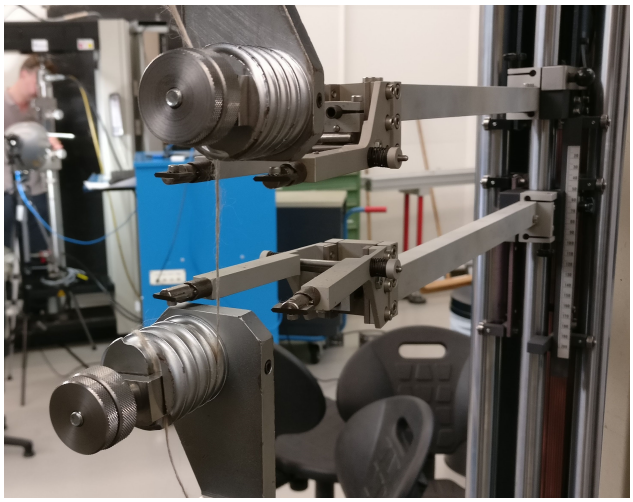

Figure 3.2: Coiled clamps utilised in the tensile test set-up for continuous fibres

The data obtained from the Zwick tensile test machine can be imported into Matlab to perform data processing. Extensometer oscillations were observed throughout the tests, and these oscillations can also be seen in the raw data as unstable force measurements at a specific strain deformation (Figure 3.3). The oscillations were not unique to one group of fibres and consistently present in all test. The most likely cause for the oscillations is the morphology of the fibres. As discussed in Section 2.2.1, the morphological structure of technical fibres consists of spun elementary fibre bundles, which are bound together by pectin. It is hypothesised that the oscillations observed by the extensometer are due to changes in load-paths as the load-bearing elementary fibre bundles change. As the load increases, the load distribution shifts the most efficient bundles in the technical fibre. Large drops in measured load can be observed at higher strains, indicating the fibre bundles carrying the load at that moment failed. The measured load increase again at a similar rate, suggesting that the next set of elementary fibre bundles picked up the load-bearing path. It may be assumed that one small fraction of all elementary fibre bundles

spun within a technical fibre are taut when the critical load is reached. The effect of the redistributing load-paths within the fibres on the determination of the tensile properties is minimised by detecting the first 7.5% force drop after the 0.25 mm elongation mark has passed. The force - displacement relationship (44.05N/mm) is determined with a linear regression line utilising the data points within the 0.25 and 0.5 mm displacement bin-width. The effect of these two processing conditions are visible in Figure 3.4.

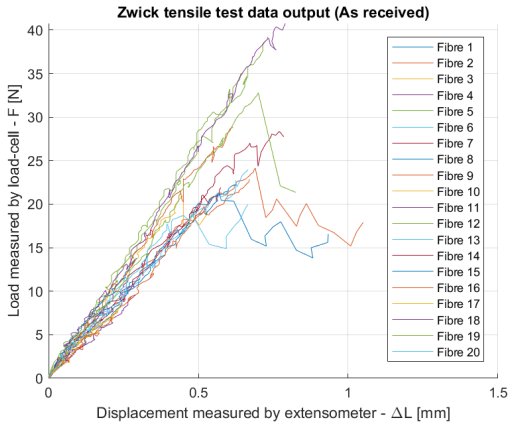

Figure 3.3: Load - displacement plot of the data output by the Zwick tensile test

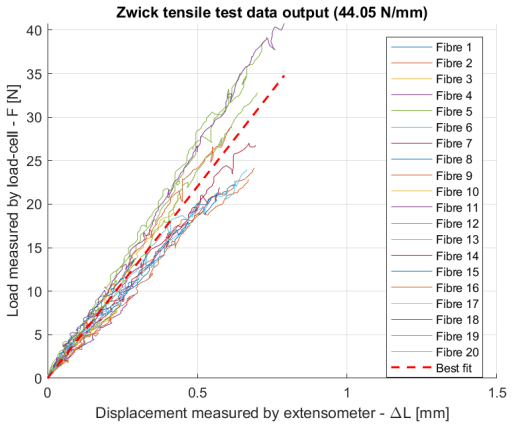

Figure 3.4: Load - displacement after processing the raw data

Verification

Verification of the mechanical properties of the fibres requires knowing the effectively active cross-sectional area of the fibre during testing. As was explained in literature, technical flax fibres are composed of woven elementary fibre bundles which are highly subject to scatter with respect to their diameter, tensile strength and E-modulus (see Table 2.1). For this reason a series of assumptions backed by literature and lab observations are required in order to establish a realistic effective load-bearing cross-sectional area (A_{eff}) which can be used to determine the tensile strength and the E-modulus of the technical fibre. The modulus is determined with a linear regression of the data points within the 0.35 and 0.85% strain deformation bin-width.

3.2. Dog-bone production and characterisation

The SFFT requires small and transparent dog-bone samples with a pre-tensioned elementary fibre spanning the specimen length along the middle. The methodology to manufacturing the samples has three main requirements. First and foremost, the matrix must be transparent in order to allow light to traverse it. Secondly, the fibre to be fragmented must taut and be placed in the middle w.r.t. to both the sample width and thickness. Finally, the distance between the fibre and the sample surface must not exceed the focal length of the required magnification lens of the microscope. The manufacturing process and dog-bone geometry (Figure 3.5) detailed on this section are largely based on the work of by Feih et al. [40]. Note that the test section length is actually 15 mm because of the 1 millimetre diameter fillet on each side.

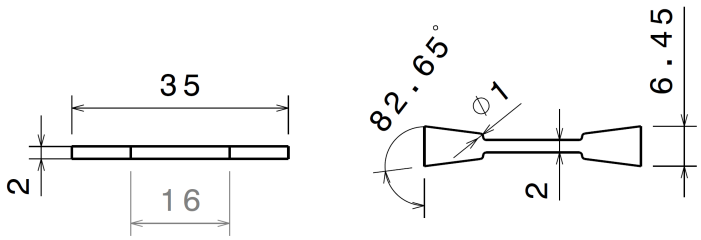

Figure 3.5: Dog-bone specimen (dimensions in millimetres)

3.2.1. Dog-bone manufacturing

The challenge in creating the samples lies in the placing the elementary fibres. The fibre needs to be pre-tensioned for two reasons aside from the fact that it needs to be taut for centring. The first is increasing

the probability the ultimate tensile stress is reached during straining, the second is to compensate for the compressive stresses that will be acting on the fibre due to the shrinkage of the polymer during curing [40]. The most suitable and simple production method is casting the epoxy into an open silicone mould.

Making the silicone mould

Silicone products are made by casting a mixture of two components (silicone rubber base and respective curing agent) into a plastic or metallic mould. The wished silicone product is a family of five dog-bone negatives with a run-out channel at half the thickness of the dog-bone negative. The run-out serves as an accurate alignment for the placement of the fibre. The run-out channel is rounded such that the lowest point is in the middle of the channel and in the middle of the thickness of the sample. Figure 3.6 shows the aluminium mould alongside the silicone product.

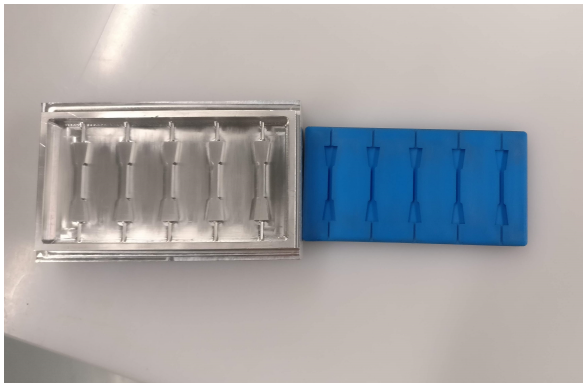

Figure 3.6: Aluminium casting mould and the produced silicone mould

Casting the SFFT samples

Normally, working with epoxy composites, is more often associated with various infusion techniques. Since a method could not be devised to manufacture samples with the use of vacuum while subjecting the fibres to a controlled level of pretension, casting remained the only viable option. For the methodology the following apparatus would be required:

1. Plastic table cover
2. One technical flax fibre
3. Silicone mould
4. 10× M12 nuts, (15.26 grams)
5. Tape
6. EPIKOTE™ Resin 04908 or EPIKOTE Resin MGS RIMR135
7. EPIKURE™Curing Agent 04908 or EPIKURE Curing Agent MGS RIMR135
8. Plastic pipette
9. Plastic beaker
10. Balance
11. Wooden stirring stick
12. Suspension beams (see Figure 3.7)
13. Eye and hand protection
14. Degassing chamber

Elementary fibres bundles (EFB) need to be manually extracted from the technical fibre (TF) while wearing latex gloves to prevent contamination from organic matter derived from the skin. The diameter and length of the EFBs can vary significantly, therefore selecting samples with similar diameters is preferable. By carefully fretting the TF, the longer and stronger EFBs will emerge by comparison to the surrounding elements. It was found that M12 nuts were suitable weights (around 15 grams) to pre-tensioned the EFB in the moulds. By adding tape to the EFB extremities they are hanged over the silicone mould within the specifically designed run-out channels while taking care of centring. In some occasions the fibre will fail due to pre-existing damage, in which case a replacement needs to be found. Tape is applied at extremities of the mould to seal off the run-out channels to prevent the epoxy from flowing out and fix the fibres in place (Figure 3.7).

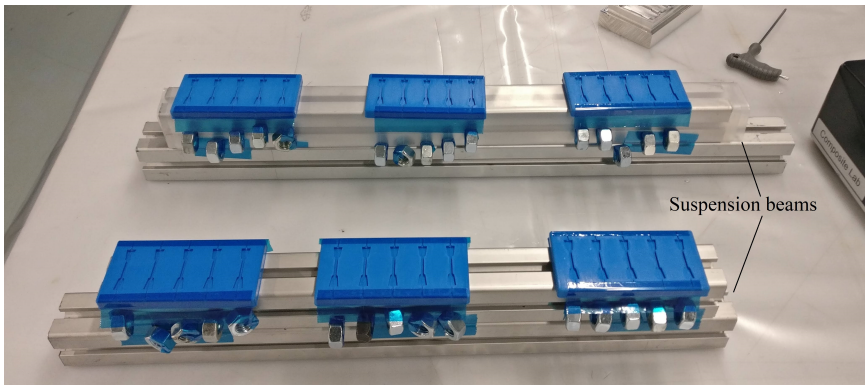

Figure 3.7: Six silicone moulds fully prepared for casting

The epoxy used to make the samples is made by mixing a 10:3 weight ratio of epoxy and curing agent in a plastic beaker. Due to the small size of the samples, 50 grams of epoxy and 15 grams of curing agent were found to be abundant for six sets of five sample moulds. After mixing the two components, they require degassing for 20 minutes before the epoxy is ready to be used for casting. The casting method was done with the aid of a pipette, being very careful not to create air-bubbles while the transferring the polymer from the beaker to the mould. Placing five drops on both sides of the sample allows the resin to flow into the test section which in practice was found to be the most effective way of preventing the formation of air bubble in test-sensitive areas. Epoxies are known to shrink while they cure. In order to prevent the samples from becoming too thin, a couple of extra drops can be added once the distributing flow in the test section has settled, using the bulge caused by surface tension as a supply (Figure 3.8). In the eventuality harmful gasses are a by-product of the curing process of the epoxy, the samples are then placed under a suction vent to cure for the first 24 hours after which they can be stored, inside their moulds, to cure for an additional 72 hours at room temperature to make sure the resin is fully hardened.

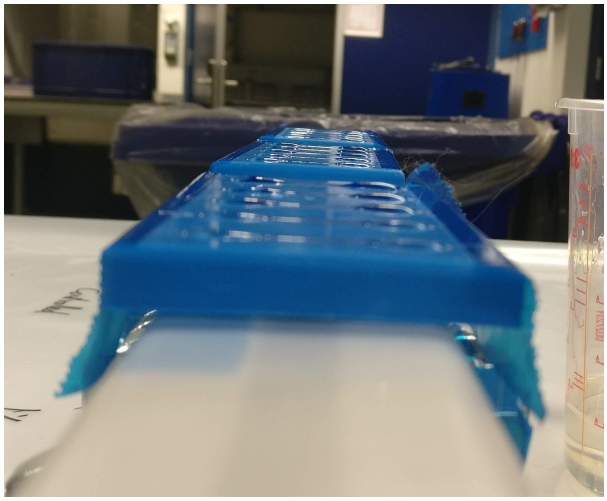

Figure 3.8: Surface tension supply of epoxy to counter shrinking during curing

Polishing the SFFT samples

Performing the SFFT requires a transparent and smooth sample allowing light to traverse it unhindered during observation. The use of a water-lubricated rotating polishing disk yielded satisfactory results. The grinding needs to be done manually, with the aid of a grinding mould to increase the control of the process and maintain an even thickness of the sample. The grinding mould is an aluminium block with sample-shaped slots on both sides (Figure 3.9). On side A the slots have a depth of 2 mm, while on side B the slots have a depth of 1.7 mm. Side A is intended to be used to remove the excessive resin residue from the casting step with 500 and 1000 grit size sandpaper. Side B is intended to polish both sides of the sample with 2000 and 4000 grit size sandpaper until no defects are visible. The final thickness of the samples was between 1.7 and 1.9 mm, which should not effect the results of the strain-based SFFT.

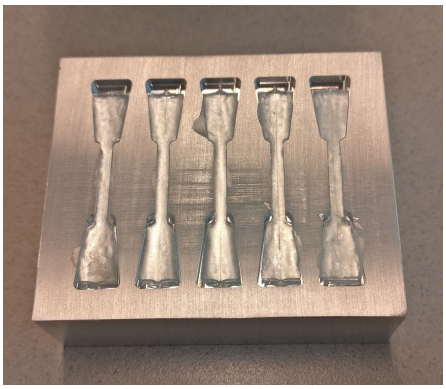

Figure 3.9: Grinding mould with 5 raw unpolished dog-bone samples

3.2.2. Dog-bone characterisation

The evaluation of the material properties of the dog-bones is essential to the strain-based SFFT. With a tensile test on the 20kN Zwick tensile machine the stress-strain relationship can be determined. The evaluation the cross-sectional area of the specimen was done with measuring caliper. In order to best approximate the testing conditions of the SFFT which relies on clamping by wedging, two metallic adaptors have been made. The adaptors can be placed in the hydraulic clamps of the tensile machine without applying any out-of-plane compression on the sample.

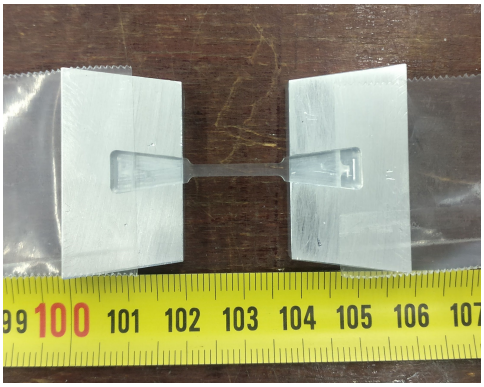

Figure 3.10: Dog-bone sample in custom made wedging grips

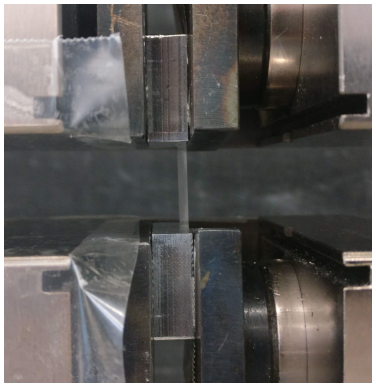

Figure 3.11: Dog-bone sample in Zwick tensile machine

A total of ten samples are tested similarly to the ASTM D638 international standard. Special grips (Figure 3.10) had to be made to test the specimen in the pneumatic clamps to avoid compressive damage in the clamping section of the specimen. A piece of tape is placed at the every extremity of the sample to prevent the parts from disassembling while placing them in the Zwick tensile machine as shown in Figure 3.11. The trapezoidal contact area assures that the sample clamps itself correctly while placing the upper grip in the machine thanks to the weight of the lower grip. A flat metal plate was used to align the bottom of the upper grip with the upper surface of the Zwick tensile machine. The bottom clamp was aligned with the grip as a result of the wedge clamping method. The hydraulic clamps are closed on both sides and pre-tensioning commences once the sample does not show any out-of-plane bending due to misalignment of the hydraulic clamps.

The Zwick software is set to reach a pre-tensioning of 10 N at a strain rate of 1 mm/min to assure that the sample is evenly loaded and not sticking to the tape. Once 10 N is reached, the strain rate switches to 0.5 mm/min to get a more accurate reading on the material response to the set strain. The program is set to end measurements once the force F on the load-cell drops below 90% of the maximum force measured $F_{\max}$. The modulus is evaluated with a linear regression of all data points within the 2 to 4% strain deformation bin-width.

3.3. Single fibre fragmentation test instrumentation and execution

The final part of this chapter treats the methodology of the SFFT. The test is performed by observing cross-polarised light traversing the dog-bone sample while it is experiencing an increasing tensile force.

The changes in stress patterns due to matrix cracking or fibre debonding are identified by the birefringence patterns (BRFPs) observed. The following methodology is influenced by the work of Feih et al. [40]. The SFFT is carried out a total of ten times per group-set as indicated in Table 3.2, with the addition of the controlled fibre group. Not all tests are successful due to premature failure, damage during sanding or air bubbles in test section, meaning that on occasion up to four different sample batches had to be made.

Table 3.2: Test-matrix – Investigated exposure times and NaOH concentrations for the single fibre fragmentation test

Treatment	30 min	45 min	60 min	90 min	120 min
1%		x			x
2%					
3%					
4%					
5%				x	
10+%					x

3.3.1. Instrumentation

Performing the single fibre fragmentation test requires the samples to be subjected to tensile stress while being observed under a microscope with cross-polarised light. A custom strain controlled tensile jig was designed and manufactured to allow this (Figure 3.12). The finest possible thread was mounted in order to minimise applied strain per full rotation of the thread. The boundary conditions imposed by the setup are the same as the ones that were made for the tensile test of the sample in section 3.2.2. Because of the similarity of the loading and the boundary conditions, the stress-strain curve obtained from the dog-bone characterisation can be used to estimate the forces and stress in the sample.

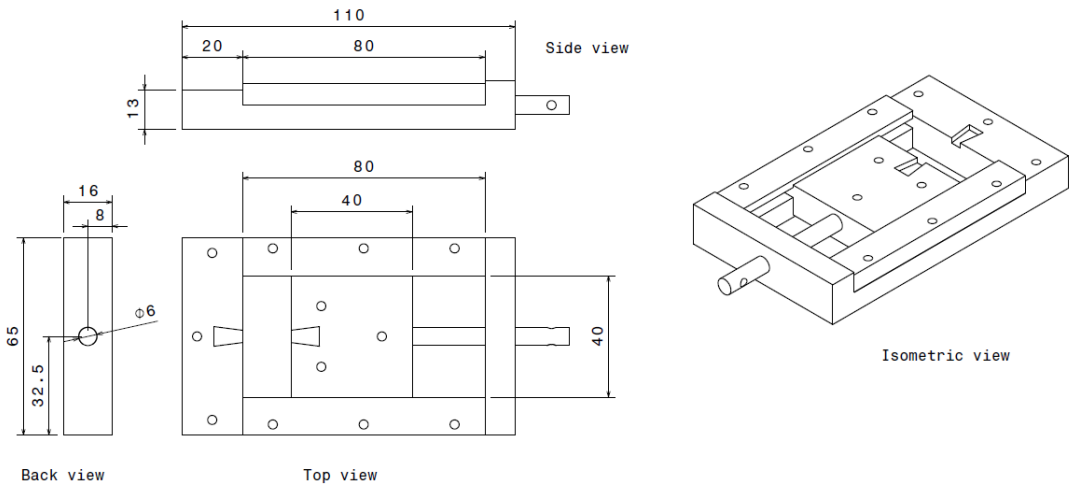

Figure 3.12: Drawing of strain controlled tensile jig (dimensions in mm)

A small silicone mould (Figure 3.13) is used to section the sample into four areas by placing marks on the sample surface with a permanent marker every 4 mm. These markings will serve as reference points when taking photos with the built in microscope camera at a 2.5×magnification. The visual range of the microscope camera at that magnification is just over 4 mm, allowing full sections to be photographed at once. Figure 3.14 shows a marked sample mounted in the strain controlled tensile jig, ready to be tested. Samples are named under the following code: p($n1$)m($n2$)b($n3$)s($n4$) where $n1$ is the NaOH percentage, $n2$ is exposure time in minutes, $n3$ is the batch number and $n4$ is the sample number (1 to 5) in that batch. Example: p1m90b2s4 is sample 4 from batch 2 that had a 1% NaOH treatment for 90m minutes.

Figure 3.13: Dog-bone sectioning for microscope orientation

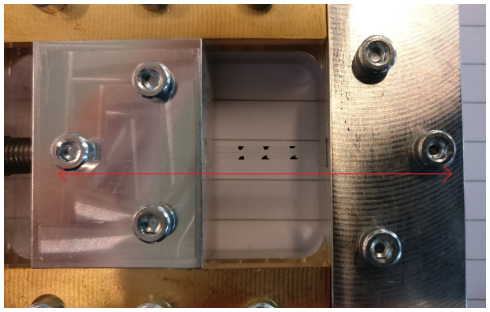

Figure 3.14: Custom made tensile jig with marked sample and calliper measured bolt distance

3.3.2. Execution of the test

Before the sample is mounted in the setup to be tested, the specimens thickness and width are measured with a caliper. Measurement should take place on the wedged section as the caliper can damage the sample by leaving a scratch on the polished surface. These dimensions are required to evaluate the stress in the sample at a given measured strain with the use of the previously evaluated stress - strain relationship.

Data collection - Basic measurements during the test

Every dog-bone sample experiences several debonds over its length. At every strain increment the amount of debonds and their lengths are measured. The data obtained can be compared to the collected test group in three ways: the total amount of debonds at saturation, the average length of the debonds at a specific strain deformation and the collective debonded length in the sample at a specific strain deformation. The data is considered valid only if the sample did not fail before reaching the plastic zone of the epoxy stress - strain curve without showing any BRFP.

Strain measurements are evaluated by evaluating the changing in distance between the two middle bolts on either side of the sample as indicated by the arrow in Figure 3.14. The unstrained aperture is determined by finding the moment the sample changes colour under cross-polarised light since that is the instance stress is introduced by the displacement. The images as seen by the camera are very dark on the default settings (10ms shutter speed) because of the cross-polarised light. Increasing the camera shutter speed to 200 - 400 ms was found to yield the best images without increasing the delay in updating the images too much on the monitor. Optimisation of colours can be further applied to increase the contrasts of the purple-green birefringence patterns. The sample is inspected under the microscope after every small stepwise strain increment that is made by turning the threaded rod. Anytime something significant changes in the appearance of the sample, the distance between the same two bolts is measured and a set of four photographs is taken for future analysis. When the sample starts reaching more critical strain, measurements and sets of photographs are made at at every strain increment to track the propagation of the BRFPs. One set of photographs is also taken after the sample has failed and is relieved of stress.

Data processing - control group

Figure 3.15 shows all the data obtained from the samples grouped into their individual sample averages. The trend-line is based on all the data points, while the averages shown indicate the average debond-length that occurred in a particular sample at a specific strain deformation. The error bars on the trend-line are based on the population standard deviation σ_p of the data points x_i w.r.t. the best-fit line μ_b that fall within the shown strain bin-width (eq. 3.1). The bin widths are equal to one tenth of the range within which sample groups have shown birefringence and N is the amount of data points present within each bin-width. Figure 3.16 shows the summation of all the debonding length within a sample at a specific strain deformation. The standard deviation is in this case taken based on the difference between the best-fit line and the summation of the debond-lengths of every sample within the shown bin-width.

$$\sigma_p = \frac{\sum_{i=1}^{N} \left[(x_i - \mu_b)^2 \right]}{N} \tag{3.1}$$

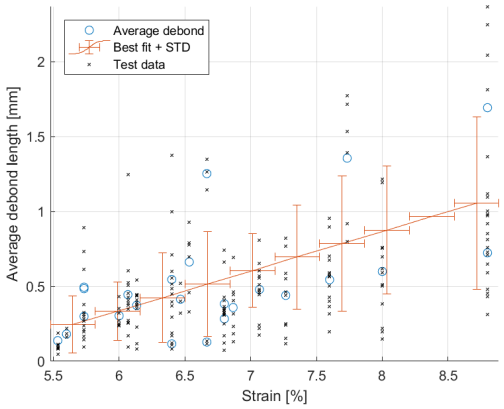

Figure 3.15: Collection of the test data of every measured debond and approximation into a linear trend line with standard deviation error bars

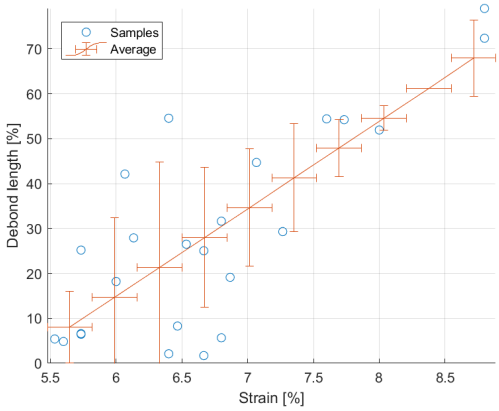

Figure 3.16: Collective debond length as measured in every sample at various strain increments with linear trend line approximation with standard deviation error bars

Data collection - Interpretation of the photographs

In synthetic fibres, fibre-cracks are detected with more easy due to their brittle failure resulting into a gap. This was found not to be the case when it comes to plant fibres. A consistent methodology for the count of fibre cracks and the measurement of interface debonding length in plant fibre SFFT was not found in literature. The following methodology is based on the observations made on unrecorded sacrificial samples which were made for the sole purpose of obtaining a better understanding of the mechanics and material interactions under tension while observed under cross-polarised light.

The first observation made was with regards to the orientation of the sample with respect to the cross-polarised light. When the two were aligned, the BRFPs around the fibre due to stress-concentrations are mainly monochromatic (Figure 3.17), whereas when the sample was rotated in plane at a small angle the patterns become diagonally symmetric green and purple (Figure 3.18). The coloured BRFPs help better establish the bounds of a specific debonded region, especially when it might start to interact with a neighbouring debond. The birefringence patterns are a result of changing refractive index in the materials and the methodology is called photoelectricity.

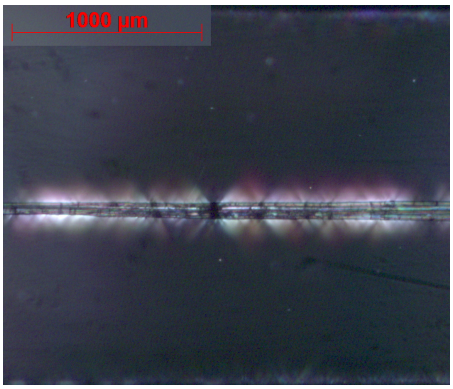

Figure 3.17: Monochromatic birefringence patterns at stress concentrations around the fibre (Type-B)

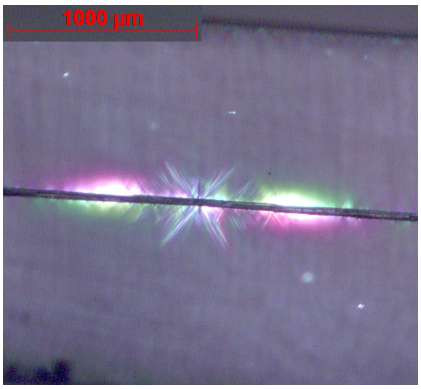

Figure 3.18: Diagonally symmetric chromatic birefringence patterns at stress concentrations around the fibre (Type-C)

The second observation confirms the concluding statements regarding SFFT made by Van de Weyenberg [23, p.224]. The BRFPs vary in shape and size depending not only on the damage the fibres may have incurred during preparation and the splitting phenomena (like in Kevlar), but also on the interaction between the two materials at the interface, *i.e.* nucleation of matrix cracks. While the size of the BRFP does increase with strain, the variation of the BRFPs make taking consistent measurements more problematic. In general, despite the variation shapes, the BRFPs can be divided into three groups: Type-A,

Type-B and Type-C. Type-A is a potential fibre failure or matrix crack with little to no debonding (Figure 3.19), Type-B is fibre failure with birefringence debonding (Figure 3.20) and Type-C is a fibre failure with debonding that only show birefringence at the extremity of the debonded area (Figure 3.21). The debonding lengths have been measured as shown in the respective figures, with the exception of Type-A since the blackening of the fibre is the only place where debonding occurs. The microscope photos have a magnification scale bar, therefore by employing a program capable of counting pixels in images will allow to determine the length of the debonds in millimetres.

Figure 3.19: Type-A: Indicates a large stress concentration due to matrix or fibre failure

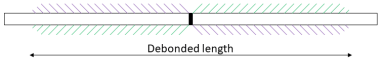

Figure 3.20: Type-B: Indicates fibre failure with birefringence debonding

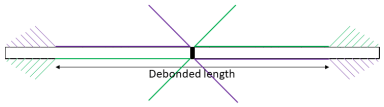

Figure 3.21: Type-C: Indicates fibre failure with debonding that only show birefringence at the extremity of the debonded area

4

Results & discussion

In this chapter the findings made during the execution of the tests and the results obtained while processing the collected data are presented. The findings presented and discussed are:

1. The effects of different NaOH surface treatments on the tensile properties of technical flax fibres.
2. The observations made regarding the execution of single fibre fragmentation test in general
3. The effects of concentration and time varying NaOH technical treatments regarding the data obtained during the single fibre fragmentation tests.

4.1. Effects of different NaOH surface treatments on the tensile properties of technical flax fibres

In this section the results obtained from investigating on the behaviour of technical flax fibres is presented. First of all the tensile properties of the controlled (as received) technical fibres are evaluated and used as a basis to verify the properties provided by the manufacturer (Bcomp). The following part compares the dependency of the tensile properties to the strength and/or duration of the alkalisation treatment.

4.1.1. Verification of the tensile properties of flax fibres

In this section the evaluated tensile properties of technical flax fibres determined and used as verification for the properties provided by the flax fibre supplier Bcomp. Figure 4.1 contains the processed data obtained from the Zwick tensile test machine, as was described in Section 3.1. A Young's Modulus of 58.90 $\pm$ 8.85 GPa has been evaluated from the linear regression of the data of 20 fibres within the 0.35 and 0.85% strain deformation bin-width, as well as an average tensile strength of 642 $\pm$ 288 MPa and an average failure strain of 1.14 $\pm$ 0.41%. The obtained results do not vary too much from the values provided by Bcomp, namely a Young's modulus of 60 GPa, a tensile strength of 800 MPa by Bcomp [42] and therefore a failure strain of 1.33%. The tensile strength seems to be significantly lower than it should be, however it was found that due to the large gauge length adopted in the test, the contribution of bundle efficiently needs to be added. The evaluation of the modulus is discussed first, followed by the effects of bundle efficiency with regards to the tensile strength.

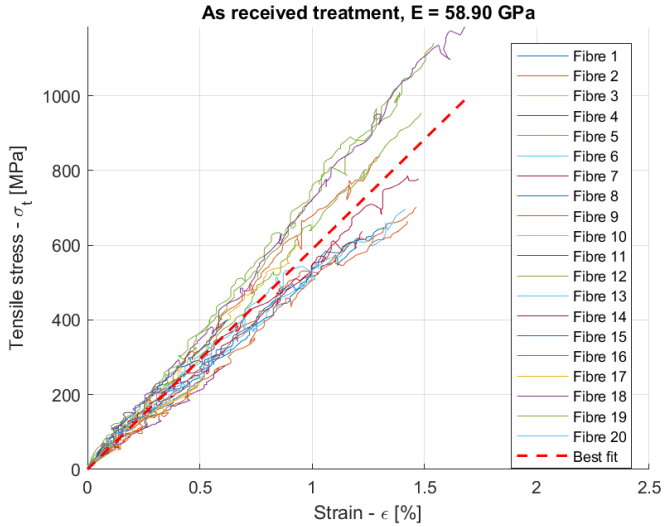

Figure 4.1: Stress - strain relationship in as received flax technical fibres with estimated modulus (control group)

Tensile stress and consequentially the Young's modulus require a cross-sectional area to be evaluated. In the methodology the effective area A_{eff} was defined as the summation of the diameters of the elementary fibre bundles that are actively engaged in the load-bearing path during the test. Given that a technical fibre from Bcomp is expected to experience around σ = 800 MPa at a strain deformation of ϵ = 1.33%, the effective area can be evaluated with eq. 4.1 to 4.3. The average gauge length L_0 at the beginning of each test after pre-tensioning was measured to be equal to 46.97 mm by the extensometer. The effective area A_{eff} results to be equal to 0.034 mm^2, which would correspond 155 elementary fibres, assuming the mean diameter is 16.8 μm [26]. From literature, it was established that anywhere between 10 an 40 elementary fibres can be found in the cross-section of an elementary fibre bundle, suggesting that anywhere between 4 and 15 elementary fibre bundles are actively bearing the load-path within the technical fibre cross-section. The evaluated effective area is considered realistic and therefore adopted for the determination of the stress - strain relationship of the tested fibres.

$$\Delta L = \frac{\epsilon \times L_0}{100\%} \qquad (4.1) \qquad F = 44.05\ \text{[N/mm]} \times \Delta L \quad (4.2) \qquad A_{eff} = \frac{F}{\sigma} \qquad (4.3)$$

The contribution of fibre bundle efficiency has been brought to light by the works of Bos et al., within which they studied the effects of the tensile properties of flax fibres depending on the gauge length of the test section [43]. Bos et al., have tested flax elementary fibres and technical fibres, the latter being subjected to a varying gauge length. They found that the Young's modulus of a technical fibre does not change as a consequence of the gauge length (Figures 4.2), however the tensile strength does significantly decrease with an increasing gauge length until it plateaus (Figure 4.3). The plateau is said to be caused by the shear failure of the weak pectin interface responsible for binding elementary fibre bundles together. When the gauge length is sufficiently small the failure mechanism changes to the cracking of the cellulose cell wall, which is significantly stronger than pectin. This is better visualised in Figure 4.4. They measured that increasing the gauge length above 25 mm reduced the fibre tensile strength to 57% of what it was evaluated to be at a gauge length of 3 mm. This is consistent with the numerical estimation of fibre bundle efficiency proposed by Wolfenden et al. [44], placing the bundle efficiency of scutched fibres at around 61% [43]. By dividing the provided tensile strength by they experimentally evaluated tensile strength, a bundle efficiency of 80% is measured, which is most likely an overestimation as a consequence of underestimating the effective contributing area.

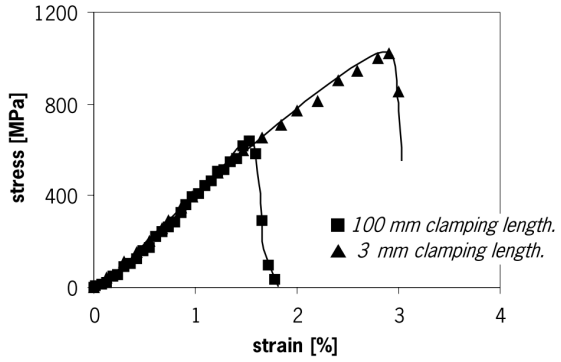

Figure 4.2: Stress - strain curves for technical flax fibres with different gauge length (gauge length) [43].

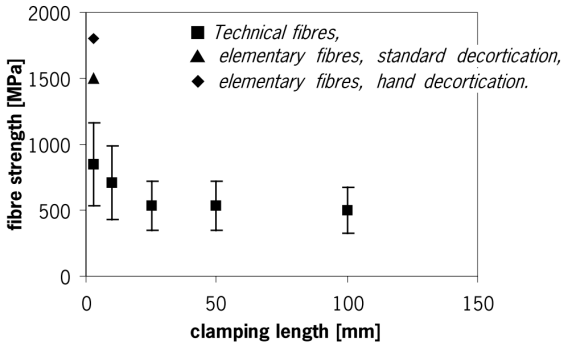

Figure 4.3: Tensile strength curve for technical flax fibres with different gauge length (gauge length) [43].

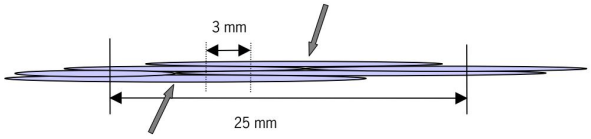

Figure 4.4: Illustration of changing failure mode due to the clamping of the elementary fibres [43].

4.1.2. The effects of NaOH concentrations and surface treatment exposure times

In this section the effects of alkalisation on the tensile properties of technical flax fibres are presented. Test variables are focussed on the NaOH concentration of the solution and the time the technical flax fibres are exposed to the solution. The methodology by which the data is precessed is unvaried for all test groups presented in the test-matrix Table 3.1. The effects of the two variables on the Young's modulus, tensile strength and failure strain are discussed in parallel to better compare their effects. Figures 4.5 to 4.7 show the collective response of the fibres to the variety of treatments they have been subjected to.

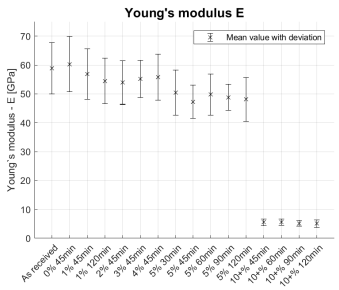

Figure 4.5: Comparing E-modulus of all test groups

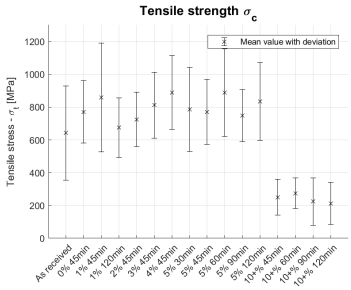

Figure 4.6: Comparing tensile strength of all test groups

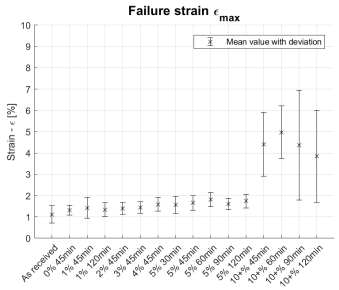

Figure 4.7: Comparing failure strain of all test groups

Effects on the Young's modulus

Starting with the concentration variable with a constant exposure time of 45 minutes, the effect of wetting the fibres can be seen in Figure 4.8 by comparing the 'as received' to the '0% 4 min' group sets. As explained in the methodology, wetting is equivalent to submerging the fibres in distilled water for 45 minutes, for consistency with the constant exposure time. Due to the very similar mean properties and standard deviation, it can be concluded that wetting and drying the fibres has no significant effect on their Young's modulus. The increase in concentration from 1 to 4% only yields a very slight of the Young's modulus, while the 5% test group observes a more sudden decrease. The addition of the 10+% treatment indicates how detrimental excessive concentrations are to the stiffness of the fibres, suggesting that the depolymerisation of cellulose occurs between concentrations of 5 and 10+%.

Figure 4.9 investigates the effects of increasing the exposure time on the Young's modulus of the fibres while the concentration is kept constant at 5%. From this comparison it can be seen that the increasing exposure time does not significantly affect the Young's modulus, while the higher percentage consistently lowered the Young's modulus in all five test groups. It is hypothesised that increasing the NaOH concentration to 6% while keeping an exposure time at 45 minutes would decrease the modulus more than increasing the exposure time from 30 to 120 min at 5% NaOH. The increased sensitivity to solution concentration is strongly suggested by the drop in properties experienced by the 10+% data group.

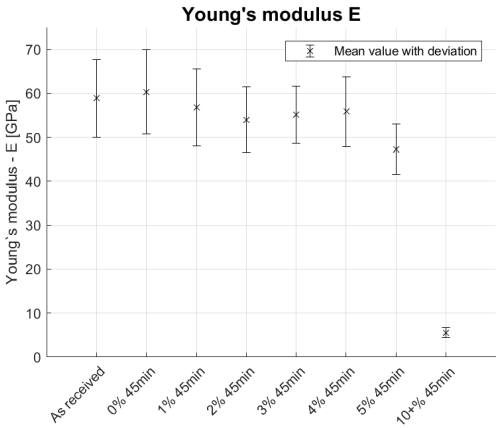

Figure 4.8: Effects of treatment concentration at 45 minutes treatment time on the fibres' Young's modulus

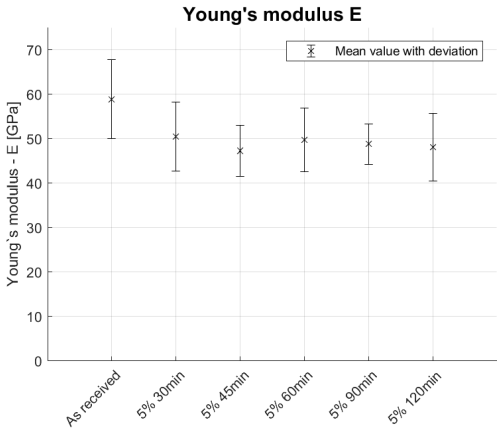

Figure 4.9: Effects of exposure time at constant 5% treatment concentration on the fibres' Young's modulus

Effects on the tensile strength

Figure 4.10 shows the changes in the tensile strength of the fibres as a result of increasing the NaOH concentration while keeping the exposure time constant at 45 minutes. Interestingly, unlike what happened with the Young's modulus, up to a concentrations of 5% the action that most affects the tensile strength is wetting and drying the fibre before testing, which results in a consistent increase of the measured tensile strength. At 10+% concentrations the tensile strength is more than halved, suggesting the possibility that a sharp decrease in tensile strength may be observed if concentrations between 6 and 10% were tested. It is likely that the loss in tensile strength is due to first the complete removal of the pectin binding the bundles together, and then the breaking down of the cellulose in the cell walls.

Figure 4.11 investigates the effects of increasing the exposure time on the tensile strength of the fibres while the concentration is kept constant at 5%. Just like with the increase in concentration, the mean tensile strength values of the treated group sets are consistently higher than the controlled group set in all cases. This once more suggests that wetting and drying the fibres before testing increases the tensile strength more than it is affected by the treatment with the used percentages and exposure times.

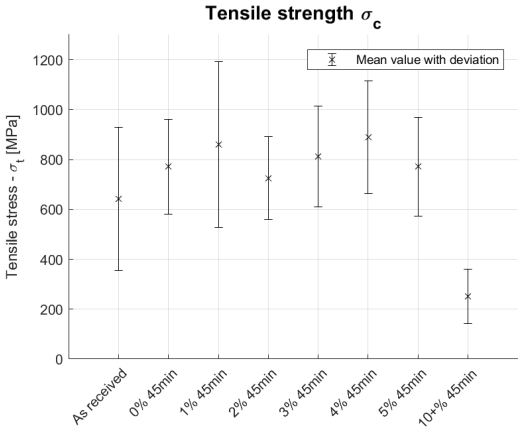

Figure 4.10: Effects of treatment concentration at 45 minutes treatment time on the fibres' tensile strength

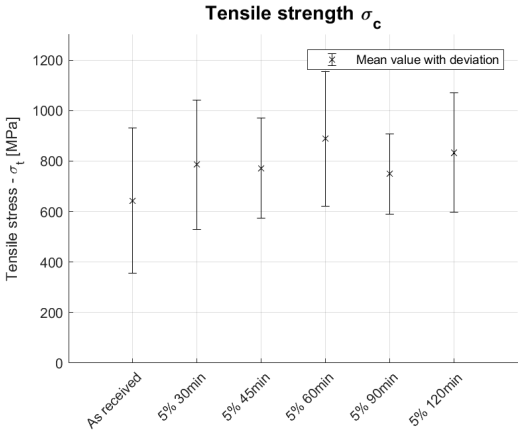

Figure 4.11: Effects of exposure time at constant 5% treatment concentration on the fibres' tensile strength

Effects on the failure strain

Figure 4.12 shows the changes in failure strain as the concentration of the NaOH solution is increased while keeping the exposure time constant at 45 minutes. By increasing the treatment concentration the fibres manage to reach higher levels of strain deformation before failing. The trend shows slight but steady increase alongside the concentration increments. Up to 5% the trend seems to be linear, however the 10+% concentration treatment shows that the failure strain becomes very large compared to the controlled. The large increase of failure strain is though to be due to the shrinking that took place in the fibres when they were exposed to the high NaOH concentration solution. From the original 1 metre fibre, crimping of up to 30% took place. The crimping was unexpected and could be an area of research in itself. It is not known whether the shrinking was unique to the technical fibre or whether the elementary fibre bundles within it were also affected.

Figure 4.13 shows the effects of increasing the exposure time on the failure strain of the fibres while keeping the concentration constant at 5%. As was determined from the concentration dependant figure, the failure strain at 5% concentration was larger than it was measured for the controlled. The time dependency once more doest not seem to further affect the failure strain.

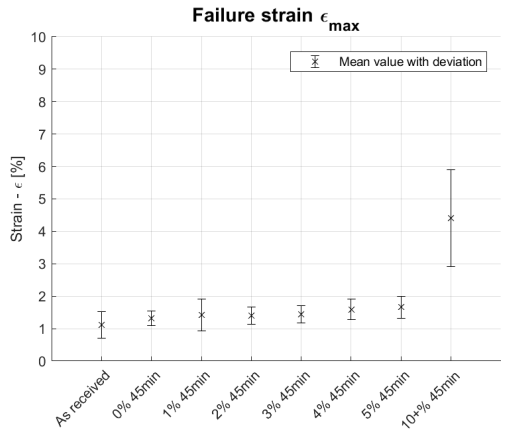

Figure 4.12: Effects of treatment exposure time on the fibres Young's modulus

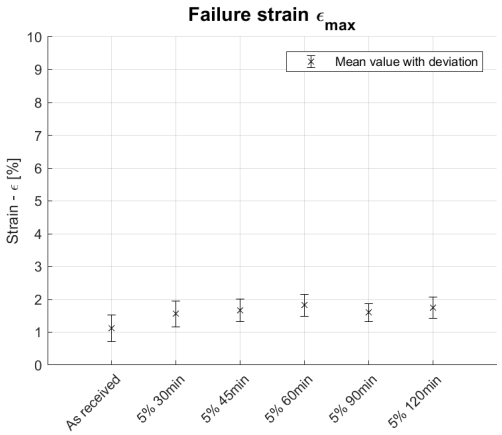

Figure 4.13: Effects of treatment exposure time on the fibres Young's modulus

Effect of excessive NaOH concentrations

In order to determine the direction in which the material responses are going as a consequence of increasing treatment concentrations, one test group has been subjected to a solution concentration larger than 10%. The most interesting observation was made immediately after submerging the fibres into the solution. The fibres visibly swelled, and as a consequence they shrank in length by 30%. Figures 4.14, 4.15 and 4.16 show the behaviour of the fibre after they were exposed to the overtreatment. The tensile modulus is decreased by more than 90% of that of the controlled. The tensile strength is significantly reduced compared to the controlled, while the failure strain is significantly increased. Shrinking is probably associated with the increasing failure strains as a consequence of increasing treatment concentrations.

Interestingly, just like with the other cases no clear trend is visible with regards to the tensile strength and the failure strain. Once more the standard deviation of the data is large any visible tend is questionable.

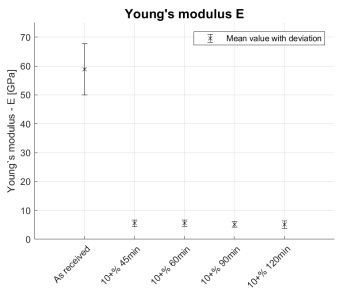

Figure 4.14: Effects of excessive treatment concentration on the fibres Young's modulus

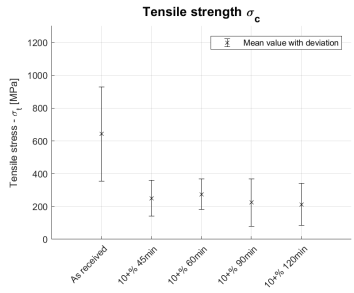

Figure 4.15: Effects of excessive treatment exposure time on the fibres Young's modulus

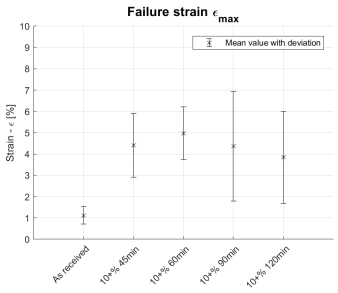

Figure 4.16: Effects of excessive treatment exposure time on the fibres Young's modulus

4.1.3. Discussion of the results regarding alkalisation of flax fibres

When considering the effects of increasing the treatment concentration or the exposure time, similar conclusions can be drawn. In both cases, the most affected parameter is the (decreasing) Young's modulus, while the tensile strength remains mostly unchanged. The decrease in Young's modulus is mainly caused by the increasing failure strain with increasing treatment concentrations. The increase in failure strain, without loss in tensile strength, is thought to be caused by the increase in elastic modulus of the fibres, led on by the decrease in MFA in the fibre bundles [18] and by the swelling-induced shrinking of the fibres that was observed during the surface treatment. In contrast to the works of Symington et al., no decrease in failure strain was observed [28, 29]

At the tested concentrations, the tensile strength seems to be unaffected as long as the pectin binding the elementary fibres together is not depolymerised. The tensile strength begins to decrease when the pectin is hydrolysed at higher concentrations, at which point also the cellulose will probably begin to degrade [8, 18]. Out of the treatment variables (concentration and time), it seems that increasing the

concentration by 1% affects the chemical composition more than an increase in exposure time. This is thought to be due to the finite quantity of solvent in the solution, leading to saturation of the reaction within the first 30 minutes. For future research it is advised to focus on increasing the concentrations at low exposure times (under 15 minutes) and attempt to detect the inflection points at which the treatment is best and when the chemical composition essential to the mechanical properties of the technical fibres begins to degrade.

In conclusion, it can be said that mechanically speaking a treatment is not favourable to the fibres since the biggest increase in properties is obtained by wetting and drying the fibres. Wetting and drying causes the fibrils in the fibres to increase their mechanical interlocking, increasing the tensile strength. This confirms what was found during the literature study, namely that the main improvements coming from the alkalisation of flax fibres arise only once within a composite by the improved adhesion. If testing of elementary fibre bundles is possible, it is advised to investigate the strain behaviour of both technical fibres and elementary fibre bundles after exposure to concentrations superior to 5% NaOH.

4.2. Tensile properties of the epoxy dog-bones

In this section the tensile properties of the epoxy dog-bones required for the interpretation of the behaviour of the single fibre fragmentation samples are presented. In the literature it was stated that the epoxy should be more elastic than the fibre in order to allow the fibres to fragment as the samples are strained. Fragmentation occurs due to the stress in the fibre exceeding its critical stress. The critical stress of flax fibres unfortunately cannot be accurately know prior to testing due to the large scatter they are prone to. Two polymers have been tested to determine which one would be more suitable for the SFFT: Standard 04908 Epoxy and the less elastic MGS RIMR135 epoxy. Both polymers have also been tested in the SFFT in order to gain understanding on the interfacial interactions between the fibre and the two different epoxies.

Figure 4.17 shows the machine test data alongside the evaluated approximation of the samples stress - strain curve into its plastic region and the Young's modulus as evaluated from the slope for the 04908 Epoxy samples. Figure 4.18 compares the performance of the two resins. The modulus of the epoxies are similar, however the failure strain of the MGS RIMR135 epoxy is approximately 2% lower. Because of the lower failure strain, the bin-width with which the modulus is evaluated has been adapted to a range from 1 to 3% strain deformation.

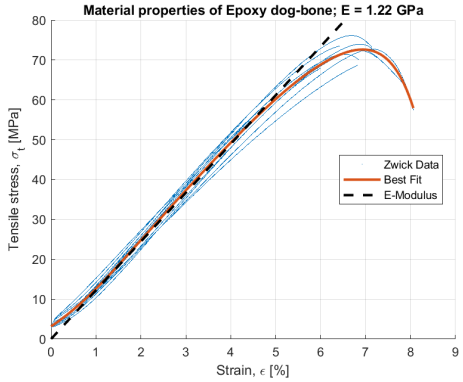

Figure 4.17: Visualisation of the Zwick data, the best-fit stress strain curve that models the boundary conditions and the determination of the Young's modulus

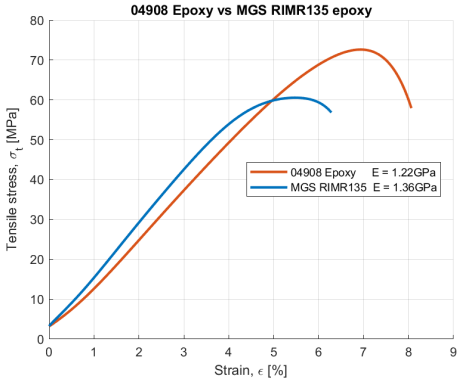

Figure 4.18: Comparing the stress - strain relationship of 04908 and MGS RIMR135 epoxy

4.3. Single fibre fragmentation test

This section focusses on the results related to the single fibre fragmentation test. Three parameters can be numerically examined when it comes to single fibre fragmentation: the average amount of debonds before failure, the average debond length in a sample at a specific strain deformation and the cumulative debond length in a sample at a specific strain deformation. Optical observations have also been made on the birefringence pattern formation and propagation, a potential indicator for the interfacial interactions between the fibre and the matrix.

4.3.1. Expected effects of improved IFSS on the SFFT

The three quantifiable parameters are relevant to understanding how the interfacial interaction between the two materials is affected by different grades of alkalisation treatment. These three parameters also used to formulate hypothesis for the expected changes in interfacial properties. The amount of debonds at saturation is an indication of the quality of the interface: Feih et al. argue that better adhesion leads to an increment of fragmentations [40]. The average debond length at a specific strain deformation (Figure 4.19) can give insight on the propagation of the debonding interface as strain is increased. The collective summation of the debond lengths (Figure 4.20) can provide information on the total debonded length as a percentage of the specimen length regardless of the amount of fragmentations.

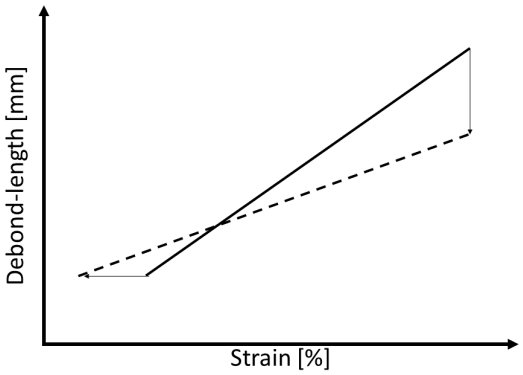

Figure 4.19: Hypothesised effect of increasing interfacial strength on the average length of the individual debonds in a SFFT sample

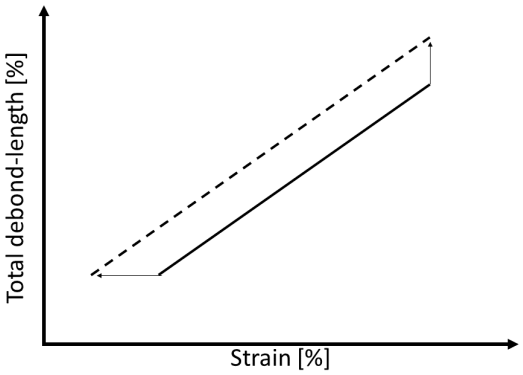

Figure 4.20: Hypothesised effect of increasing interfacial strength on the cumulative debond lengths in a SFFT sample

Increasing the interfacial strength of the fibres should, as supported by Feih et al., increase the amount of fragmentations. The amount of fragmentations can only increase if their lengths decrease. It is also thought that an improvement in adhesion should lead to fragmentations at lower strain deformations due to better shear stress transmission from the matrix to the fibres. As shown in Figure 4.19 the line is expected to decrease in gradient and begin showing debonds at lower strain deformations. Figure 4.20 instead shows an upward translation of the line because while the length of individual debonds decrease, the amount of debonds increases. The collective growth rate of the debonds should therefore not change, as the decreased growth rate of individual debonds is compensated by their increased quantity. For example: the increase in length of five small debonds at high IFSS is potentially the same as increase in length of one large debond in a low IFSS sample.

Table 4.1 shows the amount of average debonds that occurred in samples that had fibres subjected to a specific surface treatment at fragmentation saturation. Fragmentation saturation is better defined as the moment from which no new fragmentation nucleate and the debond lengths do not increase further with strain increments. The table shows that with the increasing treatment concentration and exposure time the total amount of average debonds tends to decrease compared to the as received controlled, while in the case of the lower failure strain epoxy (MGS RIMR135) the average amount of debonds increased, suggesting a better adhesion at the interface. Since a decrease in total amount of debonds with an increase in treatment is not consistent with the expected response, it is hypothesised that the increase in failure strain caused by the decrease in MFA of the elementary fibre bundles after alkalisation [18] may also be affecting the single fibre fragmentation test.

Table 4.1: Average debonds and amount of valid samples after testing

% NaOH	Minutes exposed	Epoxy	Successful samples	Average debonds
0	0	04908	10	8.9
0	0	MGS RIMR135	5	10.4
1	45	04908	7	9.0
1	120	04908	8	7.1
5	90	04908	9	7.8
10	120	04908	9	0.1

4.3.2. The effect of using a low strain failure epoxy

The controlled fibre group was also tested with two epoxies. One with a failure strain at 7%, and one with a failure strain at 5%. The stiffness of the epoxies are similar, suggesting a similarity in material response within the linearly elastic section of the stress - strain curve (Figure 4.18). Figure 4.21 compares the average debond lengths that have occurred in the two different epoxies. In the case of the low failure strain epoxy, debonds do not occur until the stress - strain peak is reached, hence in full plastic region of the epoxy. Since the fibre only fragments in the plastic region of the low strain failure epoxy, the standard epoxy is the better option to carry out the SFFT. Figure 4.22 shows the behaviour that was expected from an increase in IFSS between the epoxy and the fibre (Figure 4.20). The total debonded length in the low strain failure epoxy samples is smaller than in the standard epoxy samples, most likely because of smaller active range within which the debonds can propagate since they only initiate after the stress - strain peak of the epoxy has been reached. The debonds in the low strain failure epoxy are therefore not a result the critical stress of the fibres being reached through shear stress transfer at the interface, but by the strain incompatibility between the fibres and the epoxy. The low strain failure epoxy does reach a higher number of average debonds over the tested samples (Table 4.1), suggesting it has better adhesion with the fibre than the standard epoxy does. The hypothesised inferior adhesive properties between the standard epoxy and the flax fibres nonetheless favourable for the single fibre fragmentation test since it should lead to increased sensitivity towards changes in the IFSS between the fibre and the epoxy.

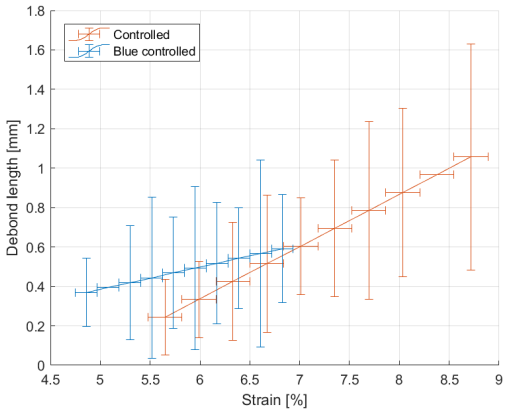

Figure 4.21: Average debond length comparison between low failure strain and high failure strain epoxy with controlled fibres

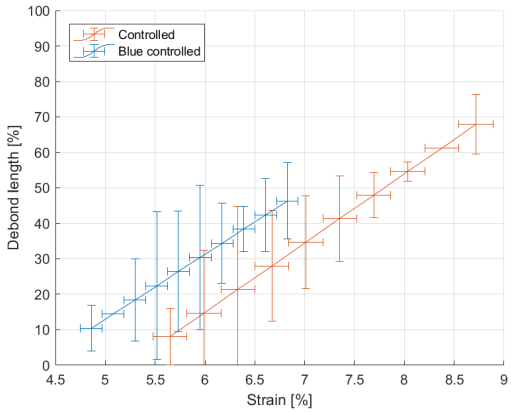

Figure 4.22: Comparison of cumulative bond length between low failure strain and high failure strain epoxy with controlled fibres

4.3.3. Effects of alkalisation on the SFFT results

In this section the effects of alkalisation treatments are compared. More specifically, the effects on the average debond length at a specific strain deformation and the cumulative debonded length at specific strain deformation. The degrees of alkalisation investigated can be found in the relative test-matrix (Table 3.2). The expected response to alkalisation has been shown in Figures 4.19 and 4.20.

Effect of alkalisation with 1% NaOH concentration on flax fibre adhesion

The single fibre fragmentation test has been performed on the test groups that have been exposed to the 1% treatment for 45 and 120 minutes. The motivation for this is to get information on the progression of the treatment over time with respect to the adhesive properties of the fibre. Figures 4.23 and 4.24 compare the effects of the respective exposure times on the average debond length in a sample with the control group, while Figures 4.25 and 4.26 compare the effects of the respective exposure times on the total debond length in a sample with the control group.

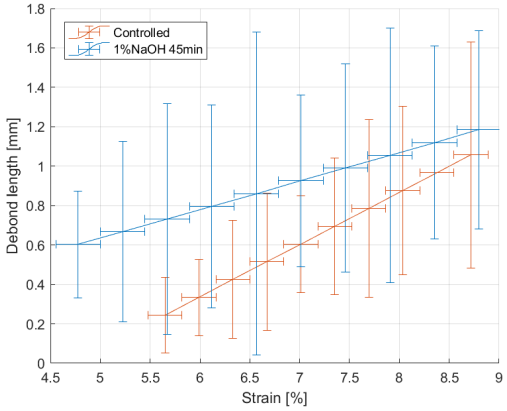

Figure 4.23: Average debond length comparison between control group and 1% NaOH - 45 min exposure time treatment

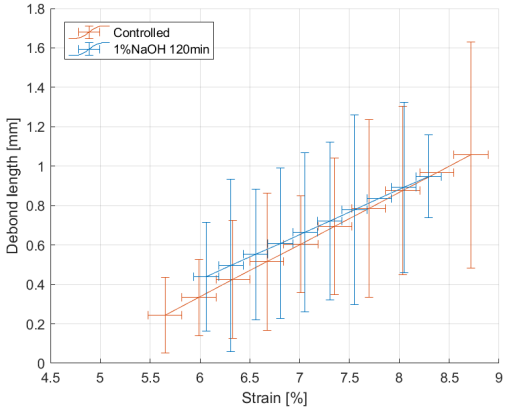

Figure 4.24: Average debond length comparison between control group and 1% NaOH - 120 min exposure time treatment

By comparing the effects of increased exposure time to the control group tests, it can be seen that especially in the case of the 45 minute exposure the behaviour expected with an increase in adhesion takes place (Figure 4.23). It is worth noting however that the error bars for this test group are very large. Nonetheless the summation of all the data points yield a trend line indicating a decrease in debond length growth rate compared to the control group and debond initiation at decreased strain deformation as would be expected of samples with improved adhesion (Figure 4.19). Figure 4.24 instead shows a similarity in behaviour between the two test groups. The range within which debonds occur in the 120 minute treated samples is however smaller than in the control group, while the rate by which the debond lengths grow is comparable both in gradient and standard deviation.

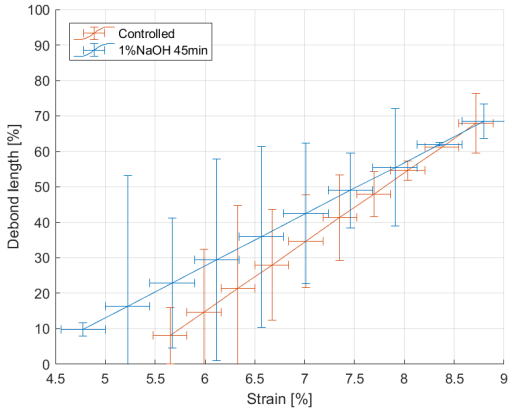

Figure 4.25: Comparison of cumulative debond length between control group and 1% NaOH - 45 min exposure time treatment

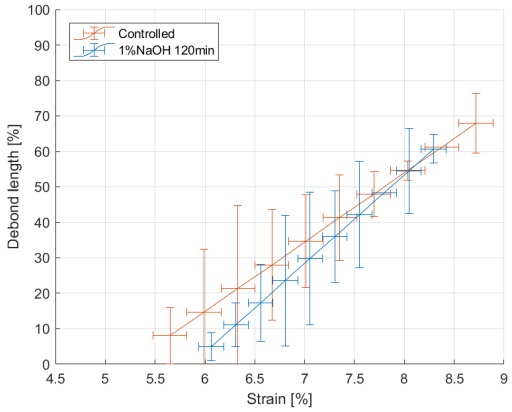

Figure 4.26: Comparison of cumulative debond length progression between control group and 1% NaOH - 120 min exposure time treatment

Figures 4.25 and 4.26 show the effect of increasing exposure time on the cumulative debond lengths progression in the samples as strain increments are made. In both cases, the trend lines converge to the control group. In the case of 45 minutes exposure, the behaviour once more matches what would be expected with an increase in adhesion of the fibres (Figure 4.20).

Effect of alkalisation with 5% NaOH concentration on flax fibre adhesion

The single fibre fragmentation test has also been performed on fibres treated with a 5% NaOH concentration for 90 minutes to observe the birefringence pattern behaviour in more critically treated samples. Figures 4.27 and 4.28 compare the average debond length of the 5% treated fibre to the controlled group and the 1% - 120 minute treatment respectively, while Figures 4.29 and 4.30 compare the cumulative

debond length of the same groups. The comparison with the 1% - 120 minute treatment is based on the possible contribution of an increased exposure time.

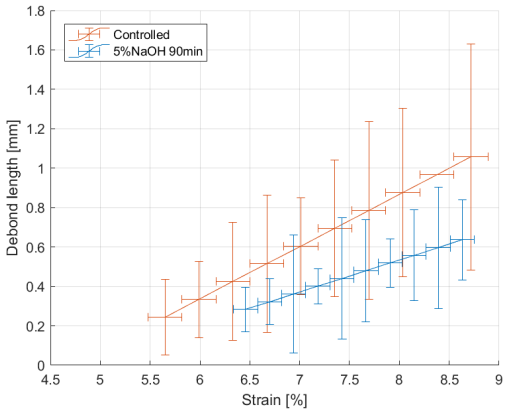

Figure 4.27: Average debond length comparison between control group and 5% NaOH - 90 min exposure time treatment

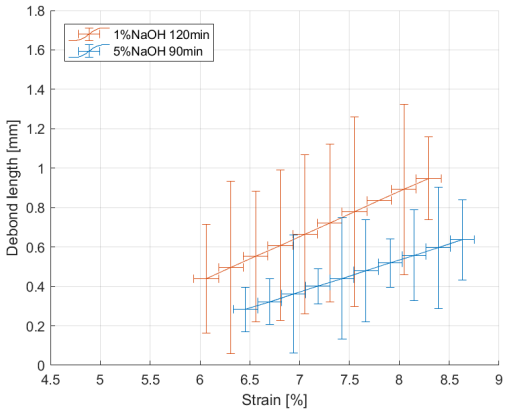

Figure 4.28: Average debond length comparison between high exposure groups with 1 and 5% treatment

Figure 4.27 compare the effect of a high concentration and high exposure time treatment (5% NaOH - 90 minute) on the adhesion of the flax fibre to the control group. The behaviour associated with an increase in adhesion (Figure 4.19) suggests that the treatment resulted in a loss in adhesion. Debonds do not occur before a strain rate of 6.5% has been reached, which is close to the stress - strain curve peak of the epoxy at 7%. A similar behaviour was observed in Figure 4.24, within which the high exposure time 1% treatment is compared to the control group. Figure 4.28 shows the similarity in strain deformation required for debond nucleation and the growth rate of the debonds of high exposure time treatments at 1 and 5% concentration. The trend lines of both the 1 and 5% treatment experience debonding at similar strain deformations and a similar rate of debond growth, suggesting that the high exposure time does affect the fragmentation test by increasing the strain deformation required for debonds to occur. The increase in treatment concentration to 5% has however resulted in a loss of adhesion, despite the fact that an improvement of the adhesion was expected.

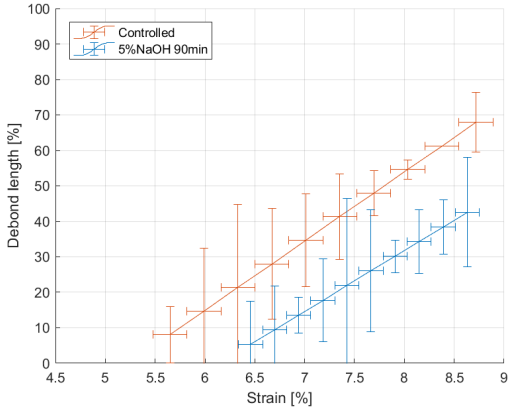

Figure 4.29: Comparison of cumulative debond length between control group and 5% NaOH - 90 min exposure time treatment

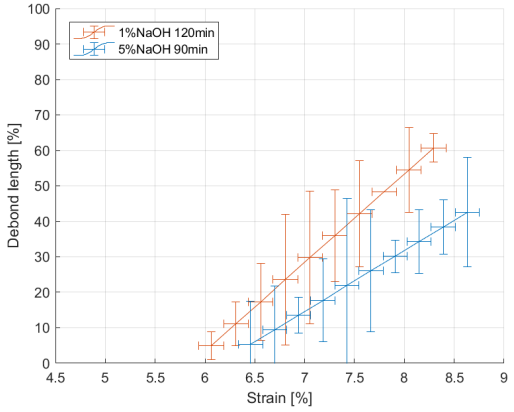

Figure 4.30: Comparison of cumulative debond length between high exposure groups with 1 and 5% treatment

Figure 4.27 shows the effect of high concentration and high exposure time treatments (5% - 90 minutes) on the cumulative debond length measured compared to the controlled group. While an improvement with respect to the adhesive properties was expected, treatment with high concentration and high exposure led to a what can be interpreted as a decrease in adhesive properties (Figure 4.20). Nonetheless, the rate by which the debonds grow is comparable to the control group. Figure 4.30 compares the

trends of cumulative debond length propagation for high exposure time treatments at 1 and 5% concentration. While the cumulative debond length is comparable at low strains, the two trend lines diverge as strain increases.

4.4. Observations made during the SFFT

The data so far presented does not sufficiently represent the mechanisms that occur at the interface between the matrix and the fibre during the single fibre fragmentation test, regardless of the treatment the fibres have been subjected to. From the analysed data, it can be observed that for increasing treatment concentration, the lines representing the average and cumulative debond growths act opposite of what was expected and depicted in Figures 4.19 and 4.20. This section focusses on the factors that could not be included in the data but were observed to have a role in the formation and propagation of the birefringence patterns, and may therefore have contributed to the unexpected behaviour of these patterns.

The section begins with an explanation of what can be seen through the microscope while performing the single fibre fragmentation test with stepwise strain increments. It was noticed that kink-bands defects and fibre diameter can affect the nucleation and propagation of birefringence patters, and their influence towards the results is also discussed. Finally, the changing properties of the fibres due to alkalisation are investigated as possible explanations for why the trend-lines describing the average debond lengths and cumulative debond length acted opposite to what was expected.

4.4.1. Visualisation of the single fibre fragmentation test

In this section the images that have been taken by the built in microscope camera are explained. Frames showing the propagation of the birefringence patterns as the strain increments increase are presented to give an idea of the difficulties associated with inhomogeneous flax fibres. The series of frames show two adjacent sections of the same sample, referred to as area 2 and area 3, with a 2.5× magnification lens. The fibre in area 2 has an average diameter of 40μm (Figures 4.31), while the fibre in area 3 has an average diameter of 90-120μm (Figures 4.32). The first set of images shows the formation of stress concentration around the fibres in both sections at a strain deformation of 4.67%. The amount of stress concentrations in area 2 are better visible and defined, while the concentrations in area 3 seem to mainly due to defects in the fibre.

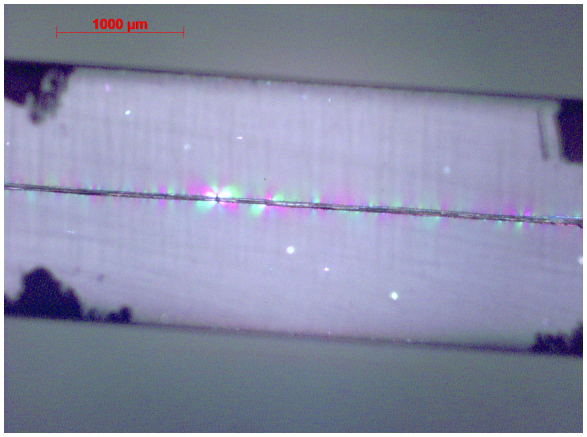

Figure 4.31: Area 2 - 4.67% strain: Formation of stress concentrations around the fibre

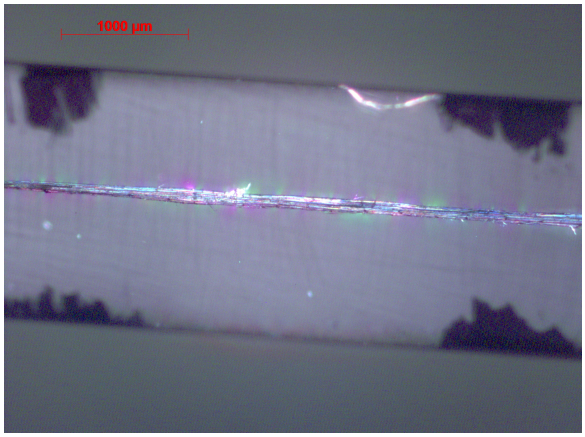

Figure 4.32: Area 3 - 4.67% strain: Fibre with larger diameter and more defects does not yet show clear stress concentrations around the fibre

A closer look at sample area 2

Figures 4.33 to 4.35 show the progression of the birefringence patterns from 5.00% to 6.33% strain deformation under 2.5× magnification, while Figures 4.36 to 4.38 show the propagation of the birefringence pattern through the same strain increments at 10× magnification. The images were taken under static loading after strain increments were manually made on the tailor made tensile jig. In some instances the birefringence patters changed while being observed under the microscope, as a consequence of relaxation of the matrix or creep. These kind of changes looked like consecutive short instantaneous snaps, increasing the length of the birefringence pattern until it became stable. The images at higher

magnification indicate that the nature of damage was matrix failure, since the fibre does not show any darkening, which was linked to fibre damage. Figures 4.44 and 4.38 show that the matrix is entering its plastic region, since the fringes on the pattern are becoming more sharp and glassy. Throughout the 10× magnification series the crack in the matrix extends perpendicularly to the fibre in both directions.

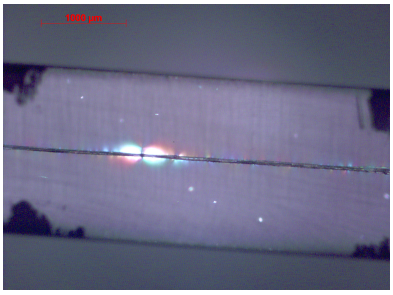

Figure 4.33: Area 2 - 5.00% strain: Nucleation of first damage leading to Type-A birefringence pattern

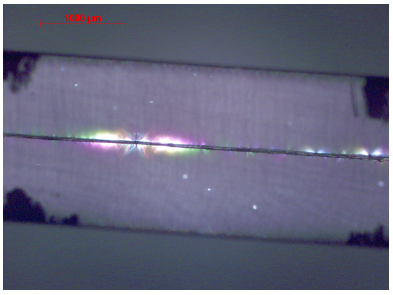

Figure 4.34: Area 2 - 5.80% strain: Debonding propagation along the fibre leading to Type-C birefringence pattern, and Type-A nucleation of new damage

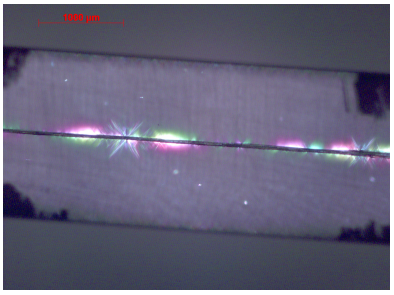

Figure 4.35: Area 2 - 6.33% strain: Debonding length increases with strain increments, signs of plasticity at matrix damage

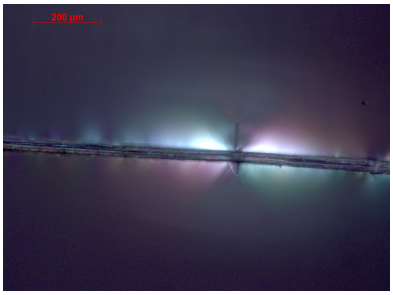

Figure 4.36: 10x magnification: Nucleation of first damage leasing to Type-A birefringence pattern (5.00% strain)

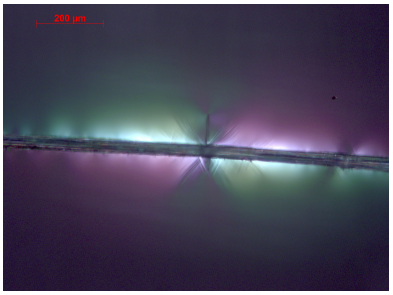

Figure 4.37: 10x magnification: Propagation of debonding (5.80% strain)

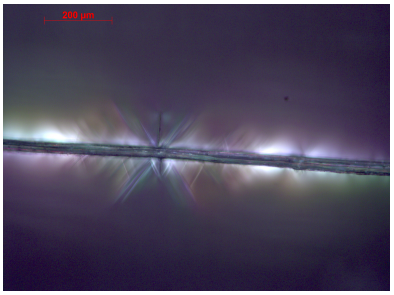

Figure 4.38: 10x magnification: Birefringence pattern showing signs of approaching the plastic zone of the epoxy (6.33% strain)

Figures 4.39 to 4.41 show sample area 2 going into the plastic region of the epoxy until failure occurs. As can be seen in Figure 4.41 the matrix crack described so far was not the cause of failure. Figure 4.39 has numbering above the three visible birefringence patterns. It is thought that BRFP 1 is caused by matrix cracking, since there is no visible darkening of the fibre and the debonding line looks more clean when compared to the other two. Birefringence patterns 2 and 3 in Figure 4.39 are thought to be due to fibre damage, since in these two cases the fibre in the middle of the pattern is darker. The crosses that are forming over the birefringence patterns are caused by the plasticity of the epoxy.

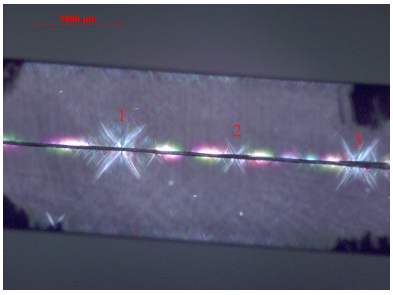

Figure 4.39: Area 2 - 6.73% strain: epoxy entering plastic zone and numbered birefringence patterns

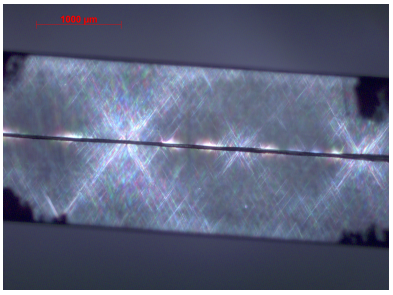

Figure 4.40: Area 2 - 7.13% strain: epoxy completely in plastic deformation, right before strain failure occurs

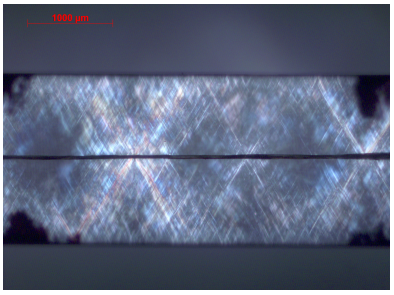

Figure 4.41: Area 2 - after failure: permanent deformation visible

A close look at sample area 3

Figures 4.42 to 4.47 show the progression of the birefringence patterns from 5.00% strain deformation to failure under 2.5× magnification. The diameter in this part of the sample is considerably larger than in area 2 showing the inhomogeneity of the fibres. While in section area 2 the birefringence patterns started showing at 5% strain deformation, in section area three they only begin to form at a strain deformation of 5.80% and become Type-B BRFPs at 6.33% strain deformation. Within the circle in Figure 4.43 a bit of darkening of the fibre is visible in the middle of the forming birefringence pattern, suggesting that it is caused by fibre damage. The darkening of the fibre follows the widening of the birefringence pattern with the increasing strain deformation imposed on the sample, and becomes clearly visible in Figures 4.45 to 4.45. The darkening of the fibre, suggesting fibre damage, remains well visible also when the load has been removed from the sample after it has failed as is shown in Figure 4.47.

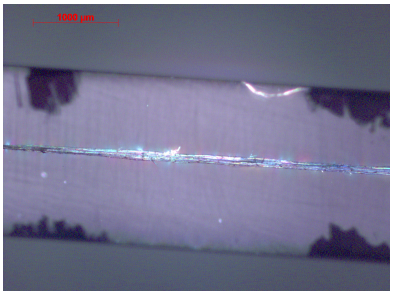

Figure 4.42: Area 3 - 5.00% strain: No stress concentrations

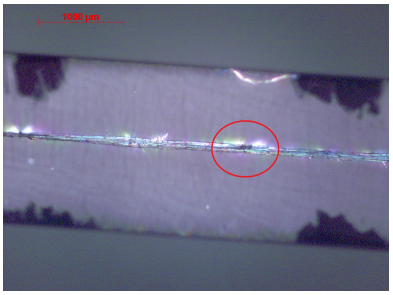

Figure 4.43: Area 3 - 5.80% strain: Stress concentration forms and fibre darkens

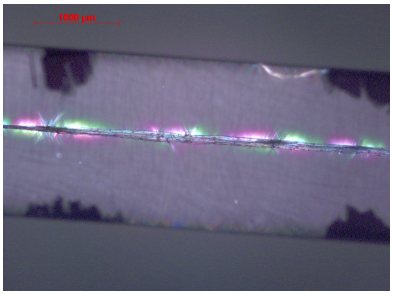

Figure 4.44: Area 3 - 6.33% strain: Stress concentrations turn into Type-B birefringence patterns with fibre darkening

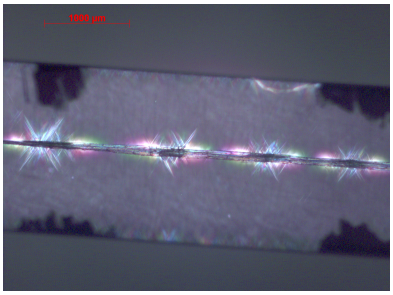

Figure 4.45: Area 3 - 6.73% strain: Visible plasticity around the birefringence patterns, fibre darkening

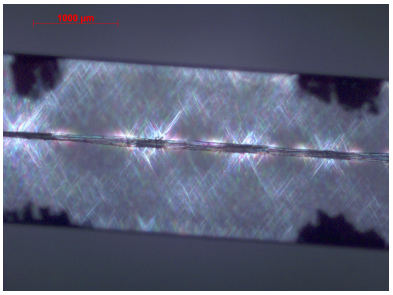

Figure 4.46: Area 3 - 7.13% strain: Plasticity of epoxy, fibre damage in good visibility

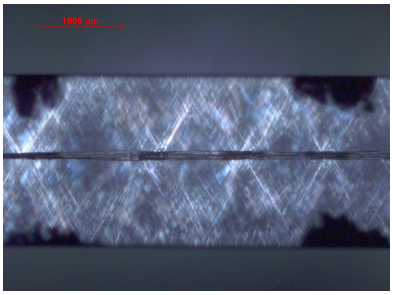

Figure 4.47: Area 3 - after failure: Fibre remains dark after load has been removed

4.4.2. Parameters affecting the formation and propagation of birefringence patterns

Formation and propagation of birefringence patterns at the fibre - matrix interface were found to de depend on the topography of the fibre. The fibre properties that were found to have most influenced the nucleation and propagation of the birefringence patterns were the diameter, the presence of kink-bands and fibre defects, and detrimental changes in the fibre chemical composition as a consequence of over-exposure or over-treatment.

Fibre diameter

Figures 4.48 and 4.49 are showing one frame of the sample that was analysed in the previous section. At a strain deformation of 6.73% the nature of the birefringence pattern was best visible in this series. The birefringence patterns have been numbered from one to six across the two section areas. As was previously mentioned, the causation of the first birefringence pattern is matrix cracking without apparent damage to the fibre, while the remaining five are thought to be caused by fibre damage. In general it was observed that low fibre diameters were more likely to propagate into Type-C birefringence patterns, whereas larger diameter fibres were more likely to manifest Type-B birefringence patterns.

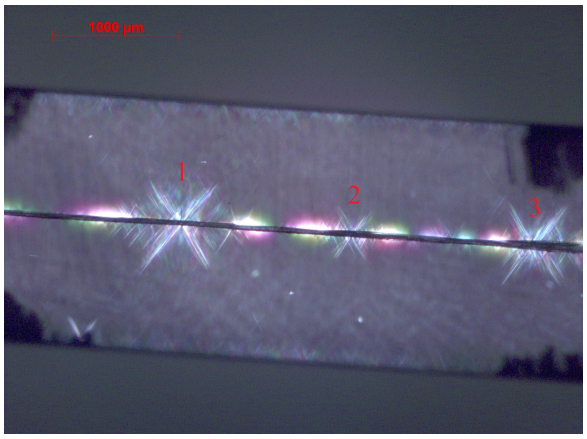

Figure 4.48: Area 2 - 6.73% strain: epoxy entering plastic zone and numbered birefringence patterns

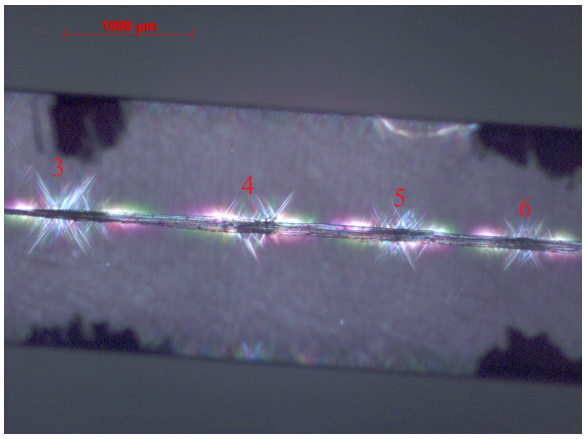

Figure 4.49: Area 3 - 6.73% strain: Visible plasticity around the birefringence patterns, fibre darkening

It is hypothesised that fibre diameter is the main responsible feature that determines whether the birefringence pattern is more likely to be caused by matrix cracking or fibre damage. Thin elementary fibre bundles are composed of fewer elementary fibres in their cross-section, probably leading to a more uniform bond with the matrix around the fibre's surface. Figure 4.50 shows a fibre with a diameter small enough to have undergone brittle failure without damaging the matrix, as would be expected to happen with glass fibre - epoxy samples [40]. As the diameter of the elementary fibre bundle increases, more elementary fibres can be found in the elementary fibre bundle's cross-section, and as a consequence a larger amount if pectin bonds is present binding the elementary fibre into a bundle. It is therefore more likely that either the pectin to fail, allowing the elementary fibres to slide and appear more dark, or a debond between the fibre and matrix to take place as in Figure 4.51 (no darkening). The diameter of the fibre is likely to affect the probability of a specific type of birefringence pattern to occur, meaning that longer debonds on large diameter fibres are still possible, just like short debonds are possible on small diameter fibres.

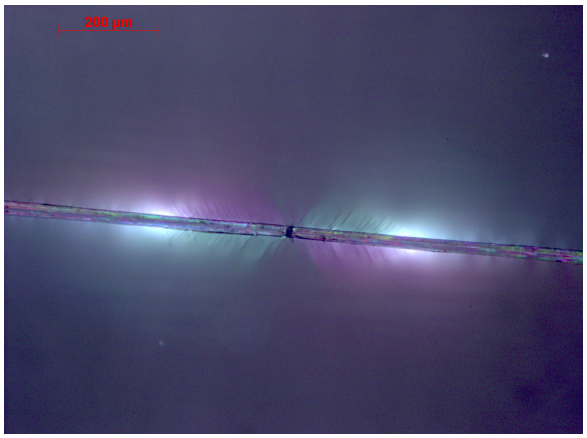

Figure 4.50: 10x magnification of brittle fibre failure at 5.60% strain deformation

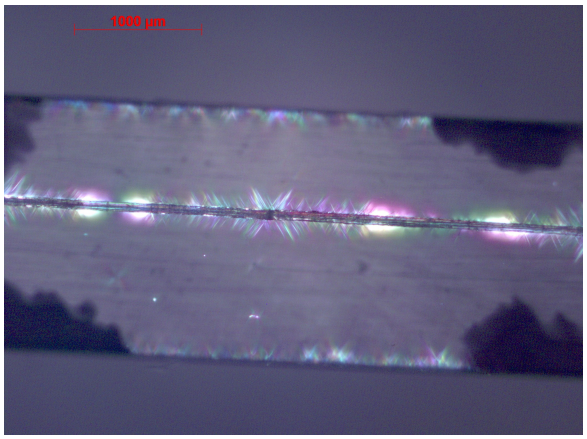

Figure 4.51: 2.5× magnification of large diameter fibre with epoxy entering plasticity, without blackening

Kink-bands and fibre defects

As was discussed in the literature section, inhomogeneity is the norm for flax fibres, and many kink-bands can be traced back to the extraction processes like scutching and hackling. Kinks-bands are better visible under the microscope with polarised light (Figure 4.52).

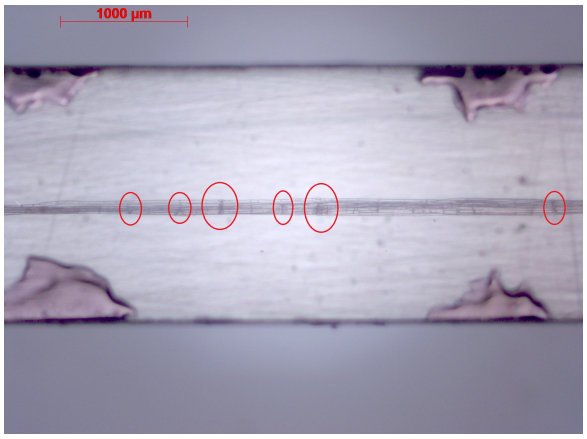

Figure 4.52: Kink-bands as seen under polarised light, unstrained sample.

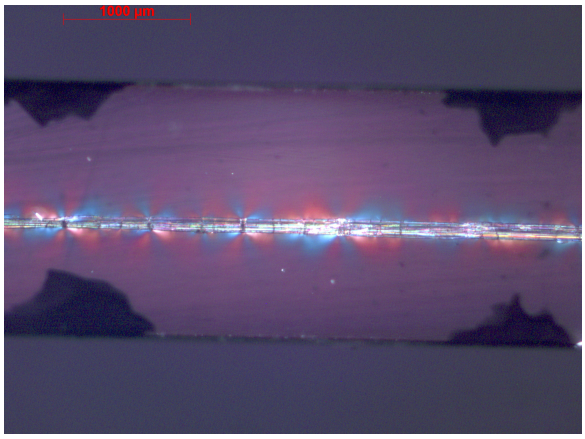

Figure 4.53: Birefringence patterns at 2.6% strain, indicating increasing stress concentrations in the matrix around the fibre kink-bands

Kink-bands serve as ideal locations for stress concentrations to form, which can lead to fibre or matrix damage. At 2.60% strain deformation the stress concentrations forming at the location where kink-bands were spotted, as can be seen in Figure 4.53. Further increments cause damage in the fibres, as can be seen from the blackening they are undergoing in the middle of each birefringence pattern (Figure 4.54). In this case measuring the size of the debonds is tricky, since they do not transition to Type-B or C from the initial Type-A.

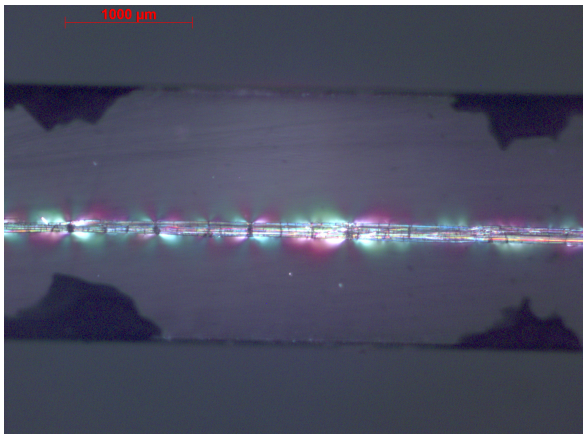

Figure 4.54: Birefringence patterns at 4.5% strain, showing the increased blackness in the fibres indicating fibre failure (Type-A)

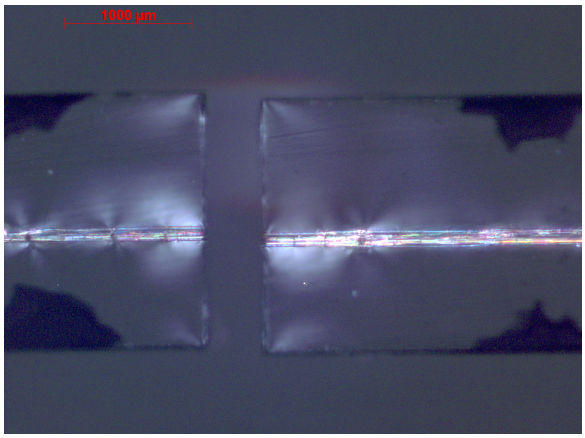

Figure 4.55: Failure caused by kink-band before reaching the plastic region of the epoxy

Defects in the fibres can act both as nucleation regions and as stopping fronts for the propagation of birefringence patterns with increasing stain increments. Figure 4.56 shows a fibre that was homogenous in diameter as well as almost deprived of kink-bands of damage. The lengths of the birefringence patterns forming around the fibre of this sample were the largest measured out of the entire acquired data. In comparison, Figure 4.57 shows the stopping qualities of defects, since defects like kink-bands have already been shown to be sources of stress concentrations. The image is taken under a static loading caused by a strain deformation of 6.60%, and the epoxy is entering plasticity.The red arrow is pointing to a lack of shear lines on the right side of the defect, while on the lower side of the fibre the shear lines are present. It was also observed that debond-stopping defects can lead to asymmetric birefringence patterns.

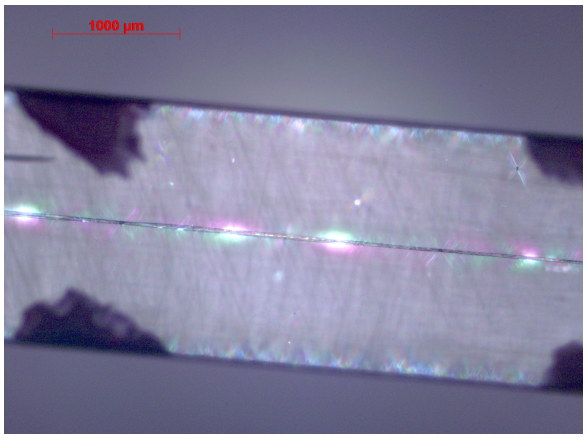

Figure 4.56: semi-homogenous fibre showing no kink-bands and brittle fibre failure with very large Type-C birefringence patterns

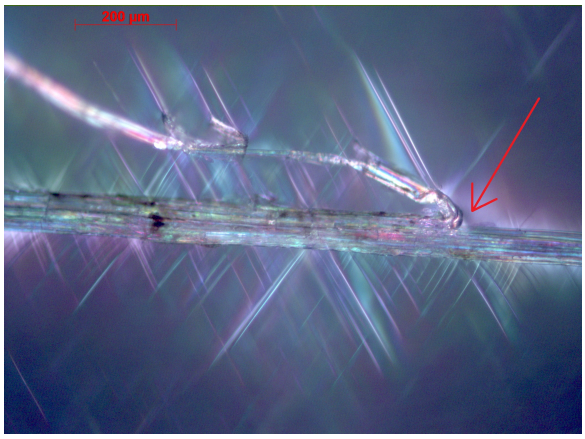

Figure 4.57: Damage stopping properties of naturally occurring imperfections

Depolymerisation

A predominant feature of the fibres that were treated with excessive concentrations (10+%) was the lack of birefringence patterns during the test. The tensile properties of the fibre were found to be similar to the tensile properties of the matrix: the epoxy had a Young's modulus of 1.22GPa and a failure strain of 7% (Figure 4.17), the over-treated fibres a modulus of $\pm$5GPa and a failure strain of $\pm$5% (Figures 4.14 and 4.16). The similarity in tensile properties means that there not enough shear loading across the interface as a result of stiffness incompatibility, which is ultimately responsible for birefringence patterns.

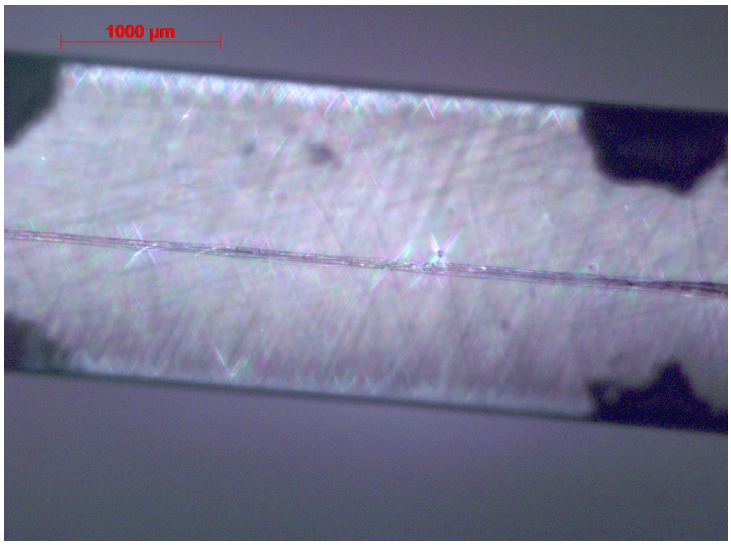

Figure 4.58: Fibre with excessive treatment - 10+% 120 minutes

Figures 4.59 and 4.60 show the debonding results analogous to the rest of the test groups. Out of all the samples tested, only one Type-A birefringence pattern formed on the fibre. The length of the debond did not increase with strain like it did in all other test groups, as can be seen from the very low gradient in Figure 4.59. Overall, the total debond length of in the samples was measured to be less that 1% Figure4.60.

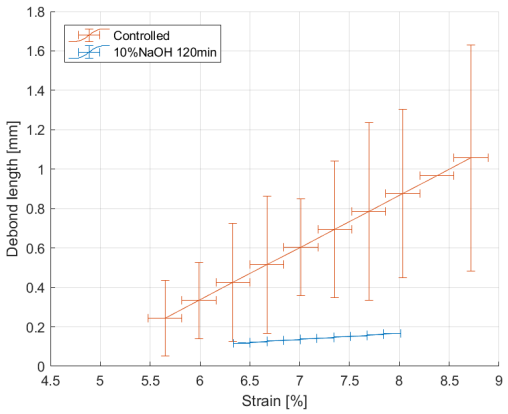

Figure 4.59: Average debond length comparison between control group and 10+% NaOH - 120 min exposure time treatment

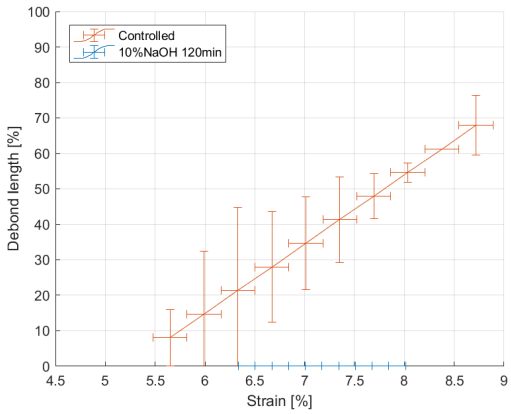

Figure 4.60: Comparison of cumulative debond length between control group and 10+% NaOH - 120 min exposure time treatment

4.5. Discussion of the SFFT results

The single fibre fragmentation test requires the modulus of the fibre to be significantly larger than that of the epoxy, and strain failure significantly lower. The disparity in tensile properties generate shear stresses at the interface which then lead to fibre/matrix damage and/or debonding. These become visible under cross-polarised light in the form of birefringence patterns thanks to photoelasticity. For these reasons the standard epoxy was selected over the low strain failure option, which was also found to have better adhesive compatibility. It was also decided that using a polymer matrix with more sensitivity to changes in interfacial shear strength was favourable to selecting the matrix with the better adhesive compatibility, since improvements in adhesion would be more noticeable. Based on the findings from literature, it was hypothesised that the single fibre fragmentation test could be applied to flax fibre in order to detect and potentially quantify the interfacial shear strength and the changes thereof as a consequence of fibre alkalisation.

In this section the hypothesis made after the literature study are compared to what was observed in the results of the single fibre fragmentation test. The main hypothesis was that an increase in adhesion would lead to an increase in fibre fragmentation and decrease of the length of the fibre fragments [40]. Due to the ductile failure of flax fibres whilst embedded in a polymer matrix (sliding of elementary fibres due to failing pectin) fragments were not detectable as they were presented in literature with studies investigating the SFFT on glass fibres. A relationship was instead found between the diameter of the fibres and the likelihood of of a Type-A birefringence pattern to transition into a Type-B or C as the strain deformation applied to the sample increases. Thin fibre were found to be more likely to display Type-C birefringence patterns while larger diameter fibres were found more likely to develop Type-B birefringence patterns. The reasoning that supports this lies in the failure mechanics of the elementary fibre bundles. Large diameter fibres are composed of more elementary fibres in the cross-section, increasing the likelihood of damage to nucleate by either matrix cracking or elementary fibres breaking the pectin bond allowing them to act individually, decreasing load-bearing efficiency. Fibre fragmentation was observed to be possible in flax fibres, provided the diameter of the fibre is small enough such that it undergoes brittle failure.

The second hypothesis that was made was relied evidence from literature supporting the idea that the poor adhesive properties of flax fibres are mostly due to the hydrophilicity of the fibres. It was hypothesised that increasing the grade of the alkalisation treatment would mainly cause the debonding vs strain deformation trend lines to act as was described in Figures 4.19 and 4.20. The expected trend-lines were observed, however acting in an inverted manner. With the exception of the 1% NaOH - 45 min sample, all other test groups displayed a trend that would, according to the hypothesis, describe a decrease in adhesion despite the fact that a larger amount of hydrophilic polymers have been hydrolysed in the longer exposure or higher solution concentration. It is therefore speculated that an additional, unexpected mechanics were affecting the results of the single fibre fragmentation test. The results of the tensile properties of the alkalised flax fibres indicated that the strain failure gradually increased with an increase in treatment strength. The increase in failure strain is due to both the effects of shrinking of

the technical fibres as a consequence of swelling and fibrillation [8], and the removal of non-structural compounds which allow the decrease of the micro-fibril angle in elementary fibres [18]. Figures 4.61 and 4.62 show the hypothesised response of increasing fibre failure strain with respect to the individual average debond-lengths and the total cumulative debond-length. It is therefore thought that a critical point regarding the chemical composition of the fibres exists, determining the behaviour of the birefringence patterns: the patterns are hypothesised to be governed at first by the changing interfacial shear strength, while after passing the critical point, the patterns are governed by the increased failure strain of the fibres. It is at this stage however not possible to quantitatively determine how much the adhesion and the elasticity have been affected by the treatment and to what extent this reflects in the birefringence patterns.

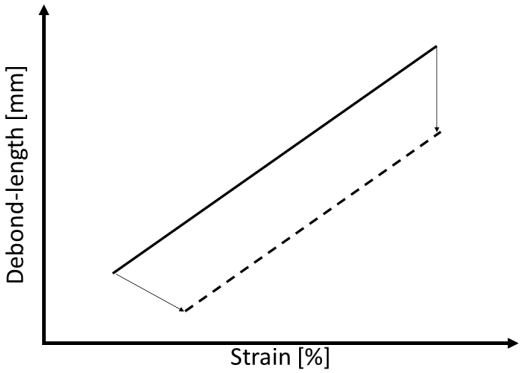

Figure 4.61: Hypothesised effect of increasing the fibre failure strain on the average length of the individual debonds in a SFFT sample

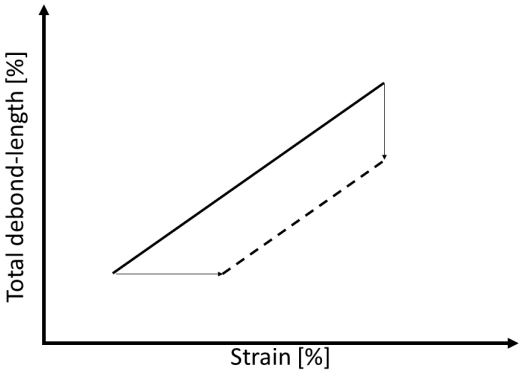

Figure 4.62: Hypothesised effect of increasing fibre failure strain on the cumulative debond lengths in a SFFT sample

Kink-bands and defects were topographical features of the fibre that were also found to significantly affect the formation and propagation of birefringence patterns. More specifically, kink-bands were almost exclusively responsible for the formation of stress concentrations at the interface, while defects could either serve as stress concentrations points or as halters for the debonding interface depending on their location with respect to other stress concentrations.

5

Conclusions and recommendations

The advance of climate change has become a greater motivator pushing forth the research of sustainable materials that are able to replace synthetic and non-degradable materials. Within the composites industry, products made with natural fibres are marketed as such to the customers, as demand for more sustainable products increases. While the durability and mechanical properties at this moment cannot yet compete with synthetic fibre composites when it comes to structural purposing, flax fibres do have the potential of replacing synthetic fibre composites in non-primary structural components and many consumer products like sports equipment or aesthetics. This concluding chapter recapitulates the main conclusions and observations made throughout the experimental research and provides answers and recommendations regarding the stated research questions. An additional section has been dedicated to recommendations that were not derived from answering the research questions.

What are the effects of sodium hydroxide treatment concentration and exposure time on the tensile properties of technical flax fibres?

Investigating the effects of NaOH treatment concentration and exposure time on the tensile properties of technical flax fibres was necessary in order to obtain a better understanding of the mechanics of technical flax fibres. The tensile tests of the treated technical fibres concluded that increasing the concentration of the treatment by 1% has a larger effect on the tensile properties than a 30 minute increment of the exposure time. It is possible that incrementing the exposure time did not affect the fibres because the finite volume solution in which the fibres had been treated had depleted its reactivity with the submerged fibres within the 30 minute exposure time. In general, the changes in tensile properties verified the work of the authors discussed in the literature section, with the exception of the effects of the treatment on the failure strain of the technical fibres. The Young's modulus and tensile strength generally decreased with increased exposure and treatment strength, and over-treatment led to a severe drop in tensile properties. Symington et al. reported a decrease in failure strain for increasing treatment exposure times [29] while the results of the tensile test indicated an increase in failure strain. It was not clear whether Symington et al. performed tests on technical fibres or on elementary fibre bundles, however it is presumed that due to the large gauge length they employed in the tensile test, technical fibres were used. Mohanty et al. wrote of an increase in elastic modulus of elementary fibre bundles as a consequence of alkalisation, which is also not in agreement with the results of the tensile tests [18]. Because of the discrepancy between the test results and the literature regarding the change in failure strain, it is recommended investigate the reaction speed of the alkalisation process to evaluate the saturation level of the reaction, and to quantify the shrinking of technical fibres after alkalisation such that it can be taken into account during the tensile tests. It is also recommended to compare the effects of alkalisation on the tensile properties of both technical fibres and elementary fibre bundles to determine the similarities and the differences between the two.

What are the effects of sodium hydroxide treatment concentration and exposure time on the adhesive properties of elementary flax fibre bundles in a single fibre fragmentation test?

Incompatibility between the flax fibres and epoxy is reported as the bottleneck of plant fibre composite performance in most studies [8, 10–12]. The incompatibility is caused by the hydrophilicity of plant fibres and the hydrophobicity of epoxy. Studies on flax fibre composites agree that the interfacial properties can be improved by alkalising the fibres, which causes the hydrophilic hemicellulose to hydrolyse, decreasing the incompatibility between the two materials. The single fibre fragmentation test was selected as the most suitable methodology to investigate the changing adhesive properties of elementary flax fibre bundles as a consequence of alkalisation because of testing conditions involving a fibre encased by epoxy, eliminating the need for high fibre strength as required in the micro-bond test or the pull-out test. Existing studies done on synthetic fibres suggested a quantitative analysis could have been performed on the changing interfacial properties by measuring the change in fragment lengths and fragmentation

intervals [40]. Based on the works done on synthetic fibres, it was hypothesised that an increase in adhesion would lead to an increase of the amount of fragments within a sample once it saturated (saturation occurs when strain increments do not cause fragmentation to increase in the sample). The model adopted for synthetic fibres was found not to be suitable for flax elementary fibre bundles because of the different failure mechanics. Synthetic fibres undergo brittle failure, making fragments clearly visible under the microscope, whereas flax elementary fibre bundles tend to undergo a more ductile failure due to multiplicity of elementary fibres composing the bundle. For this reason, it was opted to investigate the birefringence pattern nucleation and propagation patterns as an indicator of fibre - matrix debonding.

Birefringence patterns are a result of the shear stress interaction between the matrix and the fibre at the interface. The larger the difference in Young's modulus between the two materials, the faster the shear stresses will build up at the interface, causing damage in the fibre and/or the matrix. Birefringence patterns, best visible under a microscope with cross-polarised light, form at stress concentrations and at damaged locations due to the changing refractive index of the material. The is better known as photoelasticity. To allow more room with respect to strain deformation of the sample, the 7% strain failure epoxy was chosen over the 5% strain failure epoxy.

The results obtained from the SFFT with elementary fibre bundles have been compared under three aspects. The average amount of debonds that occurred in a sample after it saturated, the average length of the bonds in a sample as a function of strain deformation and the cumulative debond length in a sample as a function of strain deformation. Hypotheses based on the findings from literature predicting the behaviour of the birefringence patterns as a consequence of various degrees of alkalisation were made with respect to these three parameters. For every treatment, with the exception of the 45 minute 1% NaOH concentration, showed a behaviour contradicting the made hypotheses, suggesting additional variables were influencing the behaviour of the birefringence patterns. It was noticed that the presence of kink-bands, imperfections largely affected where the BRFPs would nucleate and how much they could propagate, the fibre diameter was found to affect the likelihood of a Type-A birefringence pattern to propagate into a Type-B or Type-C birefringence pattern and the increased strain failure of the more aggressively treated elementary fibre bundles hindered the formation of birefringence patterns due to increased strain failure similarity between the two materials. Despite the role of these variables in the formation and propagation of the birefringence patterns, alkalisation concentration and exposure time do affect the interface between the fibre and the epoxy. Kink-bands, imperfections and fibre diameters are independent variables when it comes to the effect of alkalisation on birefringence patterns, leaving changing adhesion and elasticity as the main dependant variables. It is at this stage hypothesised that a critical point should exist, indicating the transition from an adhesion governed response to a strain failure governed response as the treatment concentration and/or exposure time increases. Performing the SFFT on elementary flax fibre bundles does not yield reliable results due to the inhomogeneous nature of the fibres unless the topography of the fibres more controlled. Increasing control over the fibre selection (kink-bands, defects and fibre diameter) could potentially lead to results that do not reflect upon real flax fibre composites.

5.1. Further recommendations

In this section, the recommendations that are not directly derived from answering the research questions are presented. The most significant improvement that can be made to the single fibre fragmentation test concerns the instrumentation and the way data is recorded. Combining a tensile jig with strain gauges coupled to a recording of the entire test section under cross-polarised light would make the tests more consistent and remove the necessity for static loading while inspecting and recording images of each section. Automation of this process would allow more samples to be tested in a shorter period of time.

The alkalisation process can be improved by keeping track of the pH of the solution over the time the fibres are exposed to it, and measuring the concentration of NaOH at the end of the treatment to gain information on the reaction speed and saturation time. The selection of exposure times in the test-matrix should be based on the reaction speed relationship between the solution concentration and time the fibres have been exposed. The volume fraction between solution and fibres should remain constant. Consequentially, the tensile tests can be improved by comparing the effects the solution concentration and exposure time have on technical fibres and the elementary fibre bundles. For a more complete analysis infrared spectroscopy can be performed to evaluate how the chemical composition of the fibres changed as a consequence of the treatment. This would provide the opportunity to gather more data on the correlation between chemical composition of a fibre and its resulting mechanical properties.

Bibliography

[1] C. H. Fisher, *Journal of Macromolecular Science: Part A - Chemistry: Pure and Applied Chemistry History of Natural Fibers*, 7. 1981, pp. 1345–1375.

[2] The Editors of Encyclopaedia Britannica, *Natural fibre: Definition, Uses, and Facts*. [Online]. Available: https://www.britannica.com/topic/natural-fiber (visited on 08/30/2018).

[3] A. J. Wolfe, *Nylon: A Revolution in Textiles | Science History Institute*, 2008. [Online]. Available: https://www.sciencehistory.org/distillations/magazine/nylon-a-revolution-in-textiles (visited on 10/11/2018).

[4] M. Garside, *Global chemical fiber production from 2000 to 2018, by fiber type (in 1,000 metric tons)*, 2019. [Online]. Available: https://www.statista.com/statistics/271651/global-production-of-the-chemical-fiber-industry/ (visited on 09/22/2019).

[5] T. Johnson, *History of Composites: The Evolution of Lightweight Composite Materials*, 2018. [Online]. Available: https://www.thoughtco.com/history-of-composites-820404 (visited on 09/20/2019).

[6] V. Masson-Delmotte, P. Zhai, H. O. Pörtner, D. Roberts, J. Skea, P. R. Shukla, A. Pirani, W. Moufouma-Okia, C. Péan, R. Pidcock, S. Connors, J. B. R. Matthews, Y. Chen, X. Zhou, M. I. Gomis, E. Lonnoy, T. Maycock, M. Tignor, and T. Waterfield, Eds., *IPCC 2018: Summary for Policymakers. In: Global warming of 1.5°C. An IPCC Special Report on the impacts of global warming of 1.5°C above pre-industrial levels and related global greenhouse gas emission pathways, in the context of strengthening the global*. Geneva, Switzerland: World Meteorological Organization, 2018, p. 32, ISBN: 9789291691517.

[7] A. L. Lusher, M. McHugh, and R. C. Thompson, "Occurrence of microplastics in the gastrointestinal tract of pelagic and demersal fish from the English Channel", *Marine Pollution Bulletin*, vol. 67, no. 1-2, pp. 94–99, 2013.

[8] D. B. Dittenber and H. V. Gangarao, "Critical review of recent publications on use of natural composites in infrastructure", *Composites Part A: Applied Science and Manufacturing*, vol. 43, no. 8, pp. 1419–1429, 2012.

[9] L. Y. Mwaikambo, "Review of the history, properties and application of plant fibres", *African Journal of Science and Technology*, vol. 7, no. 2, pp. 120–133, 2006.

[10] L. Yan, N. Chouw, and K. Jayaraman, "Flax fibre and its composites - A review", *Composites Part B: Engineering*, vol. 56, pp. 296–317, 2014.

[11] D. Puglia, J. Biagiotti, and J. M. Kenny, "A Review on Natural Fibre- Based Composites — Part II", *Journal of Natural Fibers*, vol. 1, no. 2, pp. 37–68, 2004.

[12] H. Mohit and V. Arul Mozhi Selvan, "A comprehensive review on surface modification, structure interface and bonding mechanism of plant cellulose fiber reinforced polymer based composites", *Composite Interfaces*, vol. 25, no. 5-7, pp. 629–667, 2018.

[13] K. L. Pickering, M. G. Efendy, and T. M. Le, "A review of recent developments in natural fibre composites and their mechanical performance", *Composites Part A: Applied Science and Manufacturing*, vol. 83, pp. 98–112, 2016.

[14] Y. Zhou, M. Fan, and L. Chen, "Interface and bonding mechanisms of plant fibre composites: An overview", *Composites Part B: Engineering*, vol. 101, pp. 31–45, 2016.

[15] T. Huber, J. Müssig, O. Curnow, S. Pang, S. Bickerton, and M. P. Staiger, "A critical review of all-cellulose composites", *Journal of Materials Science*, vol. 47, no. 3, pp. 1171–1186, 2012.

[16] J. Summerscales, P. J. N. Dissanayake, A. S. Virk, and W. Hall, "A review of bast fibres and their composites.Part 1–Fibres as reinforcements.", *Composites Part A: Applied Science and Manufacturing*, vol. 41, no. 10, pp. 1329–1335, 2010.

[17] A. K. Mohanty, M. Misra, and G. Hinrichsen, "Biofibers, biodegradable polymers and biocomposites", *Macromolecular Materials and Engineering*, vol. 276, pp. 1–24, 2000.

[18] A. K. Mohanty, M. Misra, and L. T. Drzal, "Surface modifications of natural fibres and peformance of the resulting biocomposite: An overview", *Composite Interfaces*, no. January 2013, pp. 313–343, 2001.

[19] H. R. Carter, *Decortication of fibrous plants [Flax]*, 1913.

[20] The Editors of Encyclopaedia Britannica, *Retting - fibre-separation process*. [Online]. Available: https://www.britannica.com/technology/retting (visited on 01/16/2019).

[21] U. S. Industrial Hemp Production, "Harvesting, Retting, and Fiber Separation Retting", *Industrial Hemp in the United States*, pp. 5–8, 1998.

[22] V. Sadrmanesh and Y. Chen, "Bast fibres: structure, processing, properties, and applications", *International Materials Reviews*, vol. 0, no. 0, pp. 1–26, 2018.

[23] I. Van de Weyenberg, "Flax fibres as a reinforcement for epoxy composites", Leuven, Tech. Rep. December, 2005.

[24] A. Bourmaud, C. Morvan, A. Bouali, V. Placet, and P. Perre, "Relationships between micro-fibrillar angle , mechanical properties and biochemical composition of flax fibers", 2014.

[25] J. Summerscales and S. Grove, *Manufacturing methods for natural fibre composites*. Woodhead Publishing Limited, 2014, pp. 176–215.

[26] C. Baley and A. Bourmaud, "Average tensile properties of French elementary flax fibers", *Materials Letters*, vol. 122, pp. 159–161, 2014, ISSN: 0167577X. DOI: 10.1016/j.matlet.2014.02.030. [Online]. Available: http://dx.doi.org/10.1016/j.matlet.2014.02.030.

[27] A. Lefeuvre, A. Bourmaud, and C. Baley, "Optimization of the mechanical performance of UD flax/epoxy composites by selection of fibres along the stem", *Composites Part A: Applied Science and Manufacturing*, vol. 77, pp. 204–208, 2015, ISSN: 1359835X. DOI: 10.1016/j.compositesa.2015.07.009.

[28] M. C. Symington, O. S. David-West, W. M. Banks, J. L. Thomason, and R. A. Pethrick, "The Effect of Alkalisation on the Mechanical Properties of Natural Fibres", *Journal of Chemical Information and Modeling*, 2008.

[29] M. C. Symington, W. M. Banks, O. D. West, and R. A. Pethrick, "Tensile testing of cellulose based natural fibers for structural composite applications", *Journal of Composite Materials*, vol. 43, no. 9, pp. 1083–1108, 2009, ISSN: 00219983. DOI: 10.1177/0021998308097740.

[30] S. V. Prasad, C. Pavithran, and P. K. Rohatgi, "Alkali treatment of coir fibres for coir-polyester composites", *Journal of Materials Science*, vol. 18, no. 5, pp. 1443–1454, 1983.

[31] I. Van de Weyenberg, T. Chi Truong, B. Vangrimde, and I. Verpoest, "Improving the properties of UD flax fibre reinforced composites by applying an alkaline fibre treatment", *Composites Part A: Applied Science and Manufacturing*, vol. 37, no. 9, pp. 1368–1376, 2006.

[32] I. Van de Weyenberg, J. Ivens, A. De Coster, B. Kino, E. Baetens, and I. Verpoest, "Influence of processing and chemical treatment of flax fibres on their composites", *Composites Science and Technology*, vol. 63, no. 9, pp. 1241–1246, 2003.

[33] J. George, J. Ivens, and I. Verpoest, "Mechanical properties of flax fibre reinforced epoxy composites", *Die Angewandte Makromolekulare Chemie*, vol. 272, no. 4747, pp. 41–45, 1999.

[34] B. F. Sørensen and H. Lilholt, "Fiber pull-out test and single fiber fragmentation test - Analysis and modelling", *IOP Conference Series: Materials Science and Engineering*, vol. 139, no. 1, 2016.

[35] L. T. Drzal and M. S. Madhukar, "Fibre-matrix adhesion and its relationship to composite mechanical properties", *Journal of Materials Science*, vol. 28, pp. 569–610, 1993.

[36] H. P. S. Khalil, H. Ismail, H. D. Rozman, and M. N. Ahmad, "The effect of acetylation on interfacial shear strength between plant fibres and various matrices", *European Polymer Journal*, vol. 37, pp. 1037–1045, 2001.

[37] M. Narkis, E. J. Chen, and R. B. Pipes, "Review of methods for characterization of interfacial fiber□matrix interactions", *Polymer Composites*, vol. 9, no. 4, pp. 245–251, 1988.

[38] P. J. Herrera-Franco and L. T. Drzal, "Comparison of methods for the measurement of fibre / matrix adhesion in composites", *Composites*, vol. 23, no. 1, pp. 2–27, 1992.

[39] J. L. Thomason, "Interfacial strength in thermoplastic composites - At last an industry friendly measurement method?", *Composites Part A: Applied Science and Manufacturing*, vol. 33, no. 10, pp. 1283–1288, 2002.

[40] S. Feih, K. Wonsyld, D. Minzari, and P. Westermann, *Establishing a Testing Procedure for the Single Fiber Fragmentation Test*. 2004, p. 30.

[41] B. A. Budiman, D. Suharto, K. Kishimoto, F. Triawan, K. Takahashi, and K. Inaba, “Single Fiber Fragmentation Test for Evaluating Fiber-Matrix Interfacial Strength: Testing Procedure and Its Improvements”, *Proceeding Seminar Nasional Tahunan Teknik Mesin XV (SNTTM XV)*, no. October, pp. 809–816, 2016.

[42] Bcomp, *Technical Data Sheet - ampliTex™ Art. No. 5033 UD fabric*, Passage du Cardinal 1 / CH-1700 Fribourg / Switzerland. [Online]. Available: http://www.bcomp.ch/en/products/amplitex.

[43] H. L. Bos, *The potential of flax fibres as reinforcement for composite materials*. Eindhoven: Technische Universiteit Eindhoven, 2004, ISBN: 9038630050. DOI: 10.6100/IR575360.

[44] A. Wolfenden and S. van der Zwaag, “The Concept of Filament Strength and the Weibull Modulus”, *Journal of Testing and Evaluation*, vol. 17, no. 5, p. 292, 1989, ISSN: 00903973. DOI: 10.1520/jte11131j.